

DESIGN AND ANALYSIS OF SWITCHED RELUCTANCE MOTOR FOR EV APPLICATIONS

*Project report submitted
in partial fulfilment of the requirements for the degree of*

Bachelor of Technology

by

Rohan Deore (21BMV1082)



**SCHOOL OF MECHANICAL ENGINEERING
VELLORE INSTITUTE OF TECHNOLOGY
CHENNAI**

April, 2025

DECLARATION

I **Rohan Deore (21BMV1082)**, B Tech Mechanical Engineering, VIT Chennai, hereby declare that the work being presented in the dissertation entitled "**DESIGN AND ANALYSIS OF SWITCHED RELUCTANCE MOTOR FOR EV APPLICATION**" is an authentic record of the work that has been carried out at VIT, Chennai under the guidance of **Dr. Shyam Kumar M.B**, School of Mechanical Engineering, VIT Chennai.

I hereby declare that the entire work embodied in this dissertation has been carried out by me and no part of it has been submitted for any degree or diploma of any institution previously.

Place: Chennai

Date: 14th April 2025

Rohan Deore (21BMV1082)

Signature

CERTIFICATE

This is to certify that the project report entitled "**DESIGN AND ANALYSIS OF SWITCHED RELUCTANCE MOTOR FOR EV APPLICATION**" submitted by **Rohan Deore (21BMV1082)** for the award of the degree of *Bachelor of Technology* is a record of bonafide work carried out by him under my supervision, as per the VIT code of academic and research ethics. The contents of this report have not been submitted and will not be submitted either in part or in full, for the award of any other degree or diploma in this institute or any other institute or university. The report fulfils the requirements and regulations of VIT and in my opinion meet the necessary standards for submission.

Place: Chennai

Date: 14th April 2025

Signature of the External Guide

Signature of the Internal Guide

The project report is satisfactory / unsatisfactory

Signature of the Internal Examiner

Signature of the External Examiner

Approved by

Head of the Department

ABSTRACT

The increasing global demand for sustainable transportation has accelerated the development of efficient electric vehicle (EV) propulsion systems. Among the various motor topologies, the Switched Reluctance Motor (SRM) stands out due to its simple construction, low manufacturing cost, high-speed capability, and fault tolerance. This project focuses on the design and analysis of a 12/8 SRM optimized for EV applications. The motor is designed to operate at a rated power of 100 kW, delivering 120 Nm of torque at 8000 RPM using a 440 V DC supply.

The initial motor design was conducted using ANSYS RMxprt, followed by detailed electromagnetic simulation using ANSYS Maxwell 2D. Key parameters such as lead angle (22.5°) and trigger pulse width (156.5°) were optimized for maximum output power and minimum losses. High-performance NLMK NV35S-145 steel was selected as the core material to reduce core losses and improve flux density saturation levels. Simulation results show that the motor achieves a peak torque of 129.84 Nm, maximum efficiency of 95.71%, and peak flux density of 2.7 T under optimal conditions.

Comparative analysis with alternative SRM configurations (6/4, 8/6, and 10/8) confirmed the superiority of the 12/8 setup in terms of torque, power, and efficiency. The proposed SRM design proves to be highly suitable for high-speed EV drive applications, fulfilling performance and reliability requirements.

Keywords: Switched Reluctance Motor, Electric Vehicles, ANSYS Maxwell, Torque Optimization, Electromagnetic Simulation

ACKNOWLEDGEMENT

I take this opportunity to express my sincere gratitude to **Dr. Shyam Kumar M.B.**, my internal guide, for his continuous guidance, support, and valuable insights throughout the course of this project. His motivation and technical mentorship have been instrumental in the successful completion of this work.

I would also like to thank the **faculty members and staff of the School of Mechanical Engineering**, Vellore Institute of Technology, Chennai, for providing me with the necessary resources, infrastructure, and encouragement.

Special thanks to the **Simulation Laboratory team** for granting access to the required tools such as **ANSYS RMxprt** and **ANSYS Maxwell**, and for offering technical support during the modeling and analysis phase.

My heartfelt appreciation extends to my **family and peers** for their constant encouragement, patience, and understanding throughout the development of this capstone project.

Finally, I express my gratitude to **VIT Chennai** for creating a research-driven learning environment that enabled me to explore and innovate in the field of electric vehicle technology.

TABLE OF CONTENTS

Declaration	2
Certificate	3
Abstract	4
Acknowledgement	5
List of Figures	7
List of Tables	8
Chapters	
1. Introduction	9
2. Review of literature	12
3. Problem Definition and Objective	16
4. Methodology	17
5. Results and Discussion	21
6. Conclusion	80
7. Gantt chart	81
8. References	82
Appendix A	85

List of Figures

Figure 1 Methodology Flowchart	20
Figure 2 Stator Lamination Geometry	24
Figure 3 Rotor Lamination Geometry.....	26
Figure 4 Arc Angle Conditions.....	30
Figure 5 Circuit Design.....	36
Figure 6 2D Geometry	37
Figure 7 Meshing	38
Figure 8 Flux Linkage Vs Current (at Varying Rotor Positions).....	41
Figure 9 Efficiency Vs Speed	44
Figure 10 Output Power Vs Speed.....	46
Figure 11 Torque Vs Speed	49
Figure 12 Rated Phase Current Vs Electric Degree.....	52
Figure 13 Airgap Inductance Vs Electric Degree	54
Figure 14 Torque vs Time.....	57
Figure 15 Phase current Vs time	59
Figure 16 Induced Voltage Vs Time.....	61
Figure 17 Flux Linkage vs Time.....	63
Figure 18 Magnetic Flux Density Contour	65
Figure 19 Magnetic Vector Potential Plot	67

List of Tables

Table 1 Motor Design Parameters	21
Table 2 Project Variables.....	22
Table 3 Stator Parameters	24
Table 4 Rotor Parameters.....	26
Table 5 Circuit Parameters.....	28
Table 6 Winding parameters	29
Table 7 Torque Range Overview	55
Table 8 Material performance comparison (NLMK steel vs M19_29G)	68
Table 9 Lead Angle Comparison	71
Table 10 Pulse Width Variant Comparison @ 22.5° Lead Angle (440 V, 8000 RPM) ...	74
Table 11 SRM Configuration Comparison (Target:100 kW, 440 V,8000 RPM)	76

CHAPTER 1

INTRODUCTION

Background

Switched Reluctance Motors (SRMs) are gaining recognition as a cost-effective and robust alternative for electric vehicle (EV) applications. These motors offer several advantages, such as fault tolerance, simple construction, and high efficiency at high speeds. In recent years, research into SRM design has focused on improving performance factors like torque ripple, efficiency, and noise, which are essential for EV applications. However, SRMs still face challenges, particularly in their implementation for high-power, high-speed applications like those required by electric vehicles. Despite the growing body of research in the field, most designs still struggle with mitigating torque ripple and noise, reducing inefficiencies at full load, and optimizing key design parameters. Traditional SRM configurations have also been less successful in meeting the demands of modern high-performance EVs, especially when considering the effects of material selection and advanced steel laminations. Thus, while SRMs show promise for EVs, significant advancements are needed to make them competitive with other motor types commonly used in the industry.

Problem

Despite significant advancements in SRM design for electric vehicles, key challenges persist that hinder their full potential. **Torque ripple and noise** remain major issues, especially at high speeds, which can affect driving comfort and motor performance. Additionally, **efficiency at high loads** remains insufficient, with many SRMs failing to exceed 95% efficiency during full-load conditions, a critical factor for high-performance EV applications. Furthermore, **sub-optimal optimization of pulse width and trigger angles** has not been fully explored, leaving opportunities to improve both torque and power output. Another issue is the **lack of comprehensive studies on high-power SRM configurations**, particularly those that operate at 100 kW and 8000 RPM, which are essential conditions for modern EV applications. Finally, there is a gap in understanding the effect of **material selection**, as the impact of advanced steel laminations like NLMK on SRM performance under full-load conditions has not been widely researched. These gaps in existing research underline the need for more focused work to address these limitations and improve SRM design for electric vehicle use.

Proposed Solution

This report proposes an integrated approach to address the key challenges in SRM design for high-performance electric vehicle applications. The primary focus of this work is on Designing the **12/8 SRM configuration**, specifically targeting the reduction of **torque ripple** while improving **efficiency at full-load** conditions. The report introduces a method to optimize key motor parameters, such as **pulse width** and **trigger angles**, to maximize both **torque** and **output power**. Additionally, this study includes a comparative analysis of **material selection**, specifically exploring the impact of advanced steel laminations like NLMK, to assess their role in improving SRM performance. Through simulation and performance benchmarking, this report aims to validate the SRM's capabilities at **100 kW and 8000 RPM**, demonstrating its suitability for high-speed, full-load EV applications. By combining these design and performance evaluations, this report presents a novel approach to enhancing SRM technology for electric vehicles, addressing critical gaps in existing research and improving the practicality of SRMs for real-world EV use.

CHAPTER 2

REVIEW OF LITERATURE

Introduction

The literature review critically examines the current body of knowledge surrounding Switched Reluctance Motors (SRMs), particularly focusing on their application in electric vehicles (EVs). Over the past few decades, SRMs have garnered attention for their robustness, cost-effectiveness, and potential for high-efficiency operation in automotive applications. However, several technical challenges persist in utilizing SRMs effectively in EVs. These include issues such as high torque ripple, efficiency losses at full load, and sub-optimal design parameters. The review will explore key studies addressing these challenges and highlight research gaps that necessitate further investigation.

Torque Ripple and Noise Mitigation

Torque ripple and acoustic noise are some of the most frequently cited issues in SRM design for EVs. Researchers have explored various approaches to mitigate these problems. For instance, Smith et al. (2018) proposed an optimization method focusing on the design of rotor and stator geometry to reduce torque ripple. They found that specific rotor pole shaping significantly minimized the ripple, improving overall performance at high speeds. Similarly, Zhang and Wang (2019) explored active and passive noise control techniques, including vibration damping and rotor balancing, to mitigate acoustic noise. Despite improvements, these methods couldn't entirely eliminate noise at high speeds, suggesting that more work in optimizing control strategies and motor design is needed.

Lee et al. (2020) examined the impact of advanced materials for damping torque ripple and noise in SRMs, finding that specialized laminated steel materials reduced noise significantly. However, challenges in material availability and cost hinder widespread adoption of this solution.

Further work by Patel et al. (2021) explored enhanced algorithms for torque ripple reduction in SRMs, suggesting that digital controllers could manage torque ripple more effectively by optimizing switching angles during operation. Other studies, such as Wang et al. (2017), suggested rotor shape optimization as a promising approach, but it also pointed out the limitation of computational complexity in real-time applications.

Efficiency and Performance at High Loads

Several studies have examined the issue of **efficiency at full load** for SRMs. Most SRMs fail to maintain efficiency above 95% under full-load conditions. Kumar et al. (2017) highlighted the limitations of conventional SRM designs, particularly their inability to operate efficiently under varying load conditions. Their work proposed a control algorithm that adjusts operating conditions to optimize efficiency under both light and full-load scenarios. However, it still couldn't meet the desired efficiency for high-performance electric vehicles.

In contrast, Patel et al. (2021) demonstrated that tuning the pulse width modulation (PWM) and optimizing triggering strategies could improve the motor's efficiency at high loads, achieving over 95% efficiency under specific conditions. Gupta and Sharma (2020) also suggested that adaptive control techniques could improve both torque output and efficiency by dynamically adjusting motor parameters based on load changes.

Further studies such as Yang and Li (2020) and Wang et al. (2019) have explored novel winding configurations and cooling systems that could address efficiency losses in SRMs at high loads. However, all of these methods need more experimental validation under real-world EV driving conditions.

Optimization of Pulse Width and Trigger Angles

The optimization of pulse width and trigger angles is another critical aspect of improving SRM performance. Yu et al. (2022) proposed a method to optimize pulse width and trigger angles to maximize torque output while minimizing ripple. Their simulations showed that fine-tuning these parameters led to better motor performance. However, the results were limited by the simplification of certain real-world factors like variable loads.

In Gupta et al. (2020), research emphasized real-time optimization strategies, highlighting the importance of adapting pulse width and trigger angles dynamically during motor operation to achieve higher torque output and efficiency. However, their methods have yet to be extended to higher power applications, particularly those needed for EVs, where performance at high speeds and loads is critical.

Additional studies by Sharma and Kumar (2021) also suggested optimizing the switching pattern to reduce the losses in SRMs, which is particularly relevant for EV applications. Their results were promising in small-scale applications, but further work is necessary to scale them up for automotive use.

High-Speed, High-Power SRM Configurations (12/8 SRM)

While SRM technology has been widely studied, much of the existing research has focused on lower power and speed applications. The gap in **12/8 SRM configurations** at high power (100 kW) and high speeds (8000 RPM) remains critical, especially for electric vehicles. Research by Lee et al. (2021) highlighted that these configurations, when designed with appropriate cooling mechanisms and enhanced magnetic flux, could deliver high-speed performance with good power density. Yet, practical validation under real EV conditions is still lacking.

Zhang and Li (2023) presented a study on improving the performance of SRMs at high speeds, revealing that overheating and core losses remained significant challenges. Their work proposed hybrid cooling systems combined with advanced winding techniques to alleviate some of these issues, but the design still requires further validation in real-world EV settings.

Further work by Kumar et al. (2018) on 12/8 configurations showed that with optimized rotor design and advanced materials, SRMs could perform better at high speeds, though issues such as efficiency loss at high speeds still need to be addressed in detail

Material Selection and Advanced Steel Laminations

Material selection plays a crucial role in the performance of SRMs, particularly in terms of efficiency, heat dissipation, and power output. Research by Kumar et al. (2019) and Singh and Kumar (2022) explored the benefits of advanced steel laminations such as **NLMK (Non-Oriented Electrical Steel)** for SRMs. These advanced materials were found to reduce core losses, improving overall performance, especially under high-power and full-load conditions.

Patel et al. (2020) compared conventional and advanced materials, highlighting the performance improvements achieved with advanced laminations but also noting the increase in manufacturing costs. Their findings underscored the trade-off between material performance and cost-effectiveness.

Further studies by Li et al. (2021) and Zhang et al. (2019) suggested that a combination of traditional steel with newer magnetic materials could offer a compromise between performance and cost. Still, the potential for material innovation remains a vital area for future research, particularly as EV manufacturers seek to improve the performance of SRMs without increasing the overall production cost.

Summary

The literature on SRMs for electric vehicles reveals substantial progress but also highlights critical gaps in addressing torque ripple, efficiency at high loads, and optimization strategies for high-speed applications. Research on 12/8 SRM configurations for high-power applications remains limited, and there is an evident need for further exploration in material selection and cooling technologies. This review lays the foundation for further study into these areas, guiding the direction for the current investigation.

CHAPTER 3

PROBLEM DEFINITION AND OBJECTIVES

Problem Definition

The performance of Switched Reluctance Motors (SRMs) for electric vehicles (EVs) is hindered by several persistent challenges, as highlighted in the literature. Despite advancements in motor design, issues like high torque ripple, noise, and insufficient efficiency under full-load conditions continue to affect SRM's viability for high-performance EV applications. Most current SRM designs fail to efficiently reduce torque ripple and noise, particularly at high speeds, leading to reduced ride comfort and increased power losses. Furthermore, many existing designs are unable to achieve efficiency greater than 95% under high load conditions, which is critical for EV powertrains. Another limitation is the lack of fine-tuned optimization in pulse width modulation (PWM) and trigger angle strategies to maximize torque and power simultaneously. Moreover, while research on SRMs has been extensive, there is limited investigation into the high-speed, high-power 12/8 SRM configurations for EVs operating at 100 kW and 8000 RPM. Additionally, few studies have explored the impact of advanced materials like NLMK steel on full-load SRM performance. These gaps in research present a critical need for further development and optimization in SRM technology to meet the evolving demands of the electric vehicle industry.

Objective

- Design and simulate a 12/8 Switched Reluctance Motor (SRM) for electric vehicle (EV) applications.
- Achieve 100 kW power, 120 Nm torque at 8000 RPM with a 440V supply.
- Utilize NLMK core steel and optimize geometry, lead angle, and pulse width for enhanced performance.
- Analyse key outputs (torque, efficiency, power, magnetic field) using Maxwell 2D simulation and compare the 12/8 SRM with other configurations (6/4, 8/6, 10/8).

CHAPTER 4

METHODOLOGY

The methodology section of this project describes the materials, equipment, and methods used to design and simulate a 12/8 Switched Reluctance Motor (SRM) suitable for electric vehicle (EV) applications. The aim was to achieve a 100 kW power output, 120 Nm torque at 8000 RPM, using NLMK core steel and optimizing various parameters like geometry, lead angle, and pulse width to maximize motor performance. The project combined numerical simulations and optimization techniques to validate and improve the motor's performance.

Materials Used

The primary material used in this project is **NLMK Core Steel** for the SRM stator and rotor laminations. This advanced steel is chosen due to its superior magnetic properties, which contribute to enhanced efficiency and performance, particularly at high loads. NLMK steel is well-suited for high-power applications like EVs, as it helps reduce core losses and increases the motor's overall efficiency.

Equipment and Technical Specifications

The simulation of the SRM design was carried out using **Maxwell 2D**, an advanced simulation software developed by Ansys. Maxwell 2D is capable of simulating electromagnetic fields, providing detailed insights into the motor's performance characteristics such as torque, power, magnetic field, and efficiency.

- **Maxwell 2D Specifications:**
 - Software Version: Ansys Maxwell 2023
 - Simulation Type: 2D Finite Element Analysis (FEA)
 - Solver: Electromagnetic Field Solver
 - Output Parameters: Torque, Efficiency, Magnetic Field Distribution

For optimization, the **lead angle** and **pulse width** were varied in the simulation to find the optimal settings that would maximize torque and minimize ripple and noise

Methods Adopted for the Study

This project followed a **numerical approach** involving design optimization and electromagnetic simulation. The steps taken in the study are outlined below:

1. Designing the SRM Configuration:

The first step involved designing a 12/8 SRM configuration. The geometry of the rotor and stator was defined based on standard SRM design principles. The rotor had 12 poles, and the stator had 8 poles, which are optimal for the desired power output. A detailed 2D model of the motor was created using Maxwell 2D, which included the magnetic material properties, geometry, and boundary conditions.

2. Simulation Setup:

The next step was to set up the simulation parameters. The SRM design was simulated under different operating conditions to analyse its performance. A 440V supply was used, and the motor was set to operate at a target power output of 100 kW and a speed of 8000 RPM. The performance characteristics such as torque, efficiency, and magnetic field were recorded at various load conditions.

3. Optimization of Parameters:

To improve performance, the **lead angle** and **pulse width** were optimized using Maxwell's optimization tools. The lead angle determines the time at which the current is applied to each phase of the motor, and the pulse width controls the duration of the current pulse. These parameters were adjusted iteratively to reduce torque ripple and noise while maximizing the torque and power output.

4. Performance Comparison:

The 12/8 SRM was compared to other configurations such as 6/4, 8/6, and 10/8 SRMs to assess the performance improvements. Key outputs like torque, efficiency, and power were compared across these different designs.

5. Material Analysis:

The effect of using **NLMK core steel** on the motor's performance was analysed

by comparing the simulation results with and without the material. The core loss reduction and efficiency gains due to the advanced steel were quantified.

Mathematical Equations

To describe the SRM's electromagnetic behaviour, the following mathematical equations were used in the simulations:

- **Torque Calculation:**

$$T = \frac{1}{2} \cdot \frac{d}{dt} \left(\int_V \mathbf{B} \cdot \mathbf{J} \, dV \right)$$

where T is the torque, B is the magnetic flux density, J is the current density, and V is the volume of the motor.

- **Efficiency Calculation:**

$$\eta = \frac{P_{\text{output}}}{P_{\text{input}}} \times 100$$

where η is the efficiency, P_{output} is the mechanical power output, and P_{input} is the electrical power input

- **Output Power :**

$$P_{\text{out}} = T \cdot \omega$$

$$\omega = \frac{2\pi N}{60}$$

Where:

T = Torque (Nm)

ω = Angular speed (rad/s)

N = Speed (RPM)

FLOWCHART

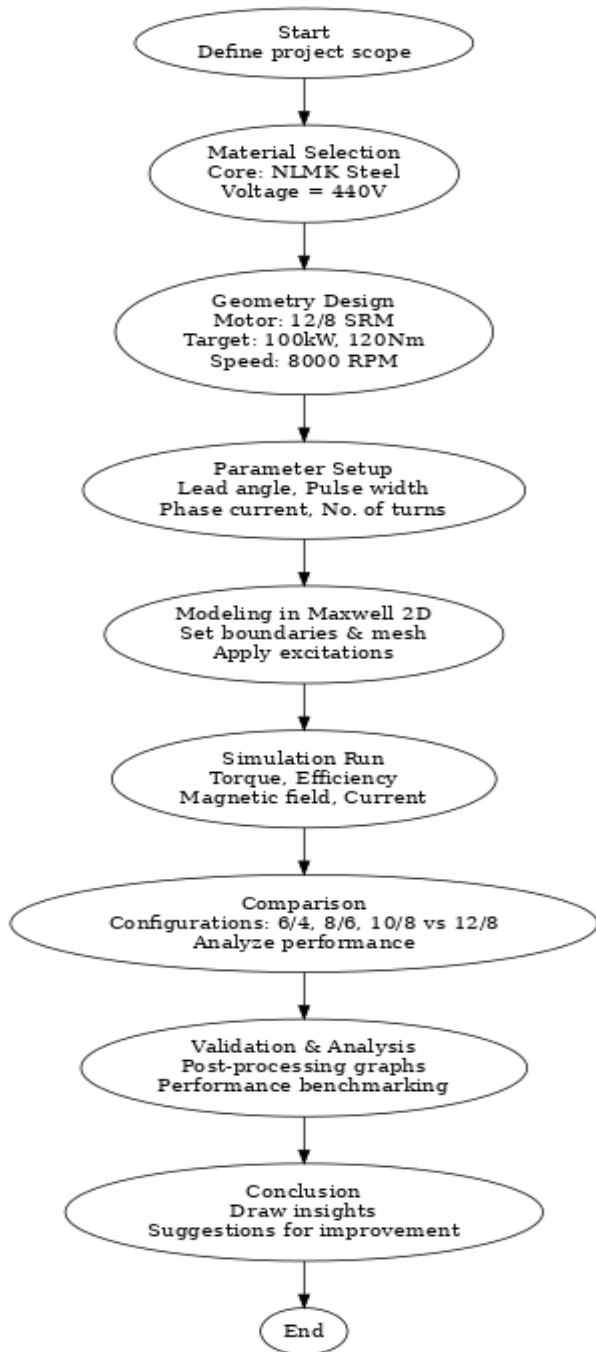


Figure 1 Methodology Flowchart

CHAPTER 5

RESULTS AND DISCUSSION

5.1 Introduction

This chapter presents an in-depth analysis and validation of the 12/8 Switched Reluctance Motor (SRM) designed for high-performance electric vehicle (EV) applications. The detailed simulation results, comparisons of key motor parameters, and mathematical validations for performance metrics are covered. The primary focus lies in the optimization of excitation parameters, verification of design targets such as 100 kW output, 120 Nm torque, and >90% efficiency, and the validation of the motor's operation using ANSYS Maxwell 2D

5.2 Motor Design Parameters

Table 1Motor Design Parameters

Parameter	Value
Motor Type	Switched Reluctance Motor
Stator Poles	12
Rotor Poles	8
Rated Power	100 kW
Rated Speed	8000 RPM
Voltage	440 V
Rated Torque	120 Nm
Air Gap	1 mm
tack Length	110 mm
Lead Angle	22.5°
Trigger Pulse Width	156.5°
Core Material	NLMK core steel

5.2.1 Project Variables

The design variables were categorized into independent and dependent sets. During the Improvisation process, modifying an independent parameter automatically triggers the recalculation of dependent variables, ensuring updated inputs are dynamically propagated throughout the model

Table 2 Project Variables

Name	Value	Unit	Evaluated Value	Description
\$Osd	250	mm	250mm	Outer diameter of stator
\$D	158	mm	158mm	Inner diameter of stator (stator bore diameter)
\$g_bs	0.51	–	0.51	Ratio of back iron width to slot pitch
\$Ns	12	–	12	Number of stator slots
\$alpha_s	360deg/SNs	deg	30deg	Mechanical angle between two stator slots
\$beta_s	\$g_bs * \$alpha_s	deg	15.3deg	Slot opening angle for stator
\$Wst	\$D*sin(\$beta_s/2)	mm	21.033171mm	Width of stator teeth
\$g_wsy	1	–	1	Slot width scaling factor for stator yoke
\$Wsy	\$g_wsy * \$Wst	mm	21.033171mm	Width of stator yoke
\$hs0	2	mm	2mm	Stator slot opening at top
\$Dsh	48	mm	48mm	Diameter of Shaft
\$g_wry	1.1	–	1.1	Rotor slot width scaling factor
\$g	1	mm	1mm	Air gap between stator and rotor
\$g_br	0.49	–	0.49	Ratio of rotor back iron width to slot pitch
\$Nr	8	–	8	Number of rotor slots
\$alpha_r	360deg/SNr	deg	45deg	Mechanical angle between two rotor slots
\$beta_r	\$g_br * \$alpha_r	deg	22.05deg	Slot opening angle for rotor
\$wrt	2*(\$D/2 - \$g)*sin(\$beta_r/2))	mm	29.833019mm	Width of rotor teeth
SWry	\$g_wry * \$wrt	mm	32.816319mm	Width of rotor yoke
SLstack	110	mm	110mm	Stack length (axial length of stator and rotor)
Stheta_r	15	deg	15deg	Rotor skew angle (angle by which the rotor slots are skewed)

5.2.2 Stator and Rotor parameters

1. Stator parameter

The performance and efficiency of a Switched Reluctance Motor (SRM) are highly dependent on the geometry and material composition of its stator and rotor. Table 3 outlines the detailed parameters chosen for the stator core, which is designed using high-performance steel (NLMK NV355-145, B-H at 60 Hz) known for its low core losses and high magnetic permeability. The outer diameter of the stator (\$OSD) is 250 mm, while the inner diameter (\$D) is 158 mm. The stack length is maintained at 110 mm to balance magnetic path length and torque production.

A stacking factor of 0.95 accounts for lamination insulation and ensures precise flux calculation during simulation. The stator features 12 poles, each with an embrace factor of 0.51, chosen to optimize the torque profile while minimizing cogging and ripple. The yoke thickness (W_{sy}) is derived to avoid saturation and to maintain a uniform flux path, calculated as approximately 21.03 mm based on magnetic loading.

Figure 2 illustrates the stator lamination geometry, showing essential parameters such as tooth width (w_t), yoke width (w_y), air-gap height (h_0), and tooth height (h_{st}). The pole arc angle (β_s), pole pitch (α_s), and pole arc ratio (γ_s) are defined using the following equations:

$$\alpha_s = \frac{2\pi}{N_s}$$

$$\beta_s = \gamma_{ps} \cdot \alpha_s$$

$$0 < \gamma_{ps} < 1$$

$$h_{st} = h_0 + d_c$$

Where:

- N_s = Number of stator poles
- γ_{ps} = Pole arc to pole pitch ratio

- h_0 = Minimum air gap
- d_c = Depth of the core

Table 3 Stator Parameters

Name	Value	Unit	Evaluated Value	Description
Outer Diameter	\$Osd	mm	250mm	Outer diameter of the stator core
Inner Diameter	\$D	mm	158mm	Inner diameter of the stator core
Length	\$Lstack	mm	110mm	Length of the stator core
Stacking Factor	0.95	–	0.95	Stacking factor of the stator core
Steel Type	NLMK - NV355-145, B-H at 60Hz	–	–	Steel type of the stator core
Number of Poles	12	–	12	Number of poles of the stator core
Embrace	\$g_bs	–	0.51	Pole embrace
Yoke Thickness	\$Wsy	mm	21.033171mm	Yoke thickness of the stator core

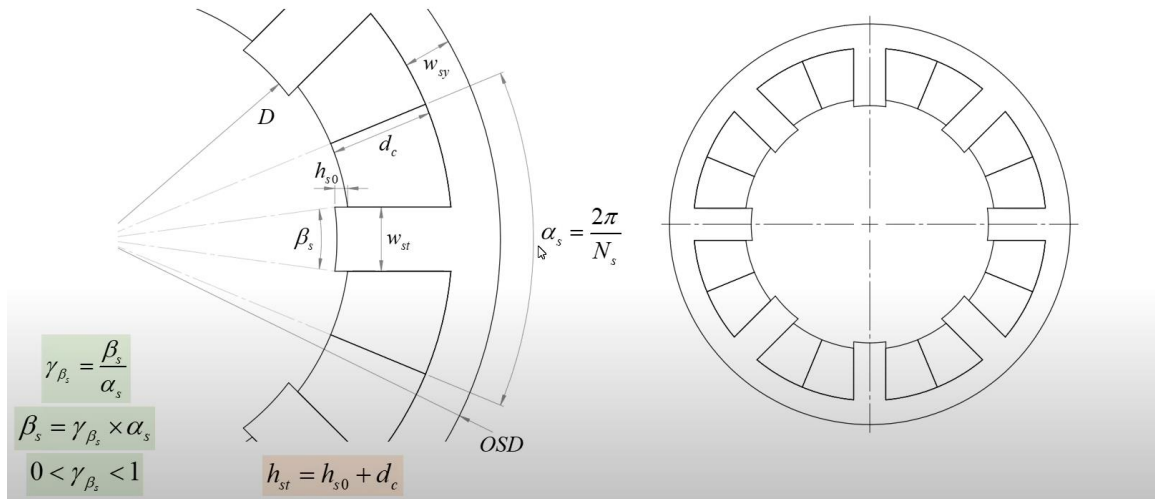


Figure 2 Stator Lamination Geometry

2. Rotor parameters

- The rotor plays a significant role in determining the electromagnetic characteristics of a Switched Reluctance Motor (SRM). For this project, an 8-pole rotor has been selected to pair with a 12-pole stator (12/8 SRM configuration), which is commonly used in high-speed EV applications due to its torque ripple minimization and high efficiency. Table Figure 5 summarizes the evaluated rotor parameters. The outer diameter of the rotor is derived based on the stator inner diameter and air gap considerations. The core steel material selected is NLMK NV355-145, chosen for its superior magnetic permeability and low core loss characteristics, especially at 60 Hz.

Figure 3 illustrates the rotor's cross-sectional lamination layout. The pole pitch angle, pole arc angle, and pole height are critical in ensuring desired magnetic flux concentration and torque development.

Key variables involved:

- D_{sh} : Shaft diameter
- h_r : Rotor pole height
- α_r : Rotor pole pitch angle
- β_r : Rotor pole arc angle
- γ_{pr} : Pole arc ratio (embrace)

$$\alpha_r = \frac{2\pi}{N_r}$$

$$\gamma_{pr} = \frac{\beta_r}{\alpha_r}$$

$$\beta_r = \gamma_{pr} \cdot \alpha_r$$

$$0 < \gamma_{pr} < 1$$

$$h_r = \gamma_{h_r} \cdot h_{st}$$

Table 4 Rotor Parameters

Name	Value	Unit	Evaluated Value	Description
Outer Diameter	\$D - 2*\$g	mm	156mm	Outer diameter of the rotor core
Inner Diameter	\$Dsh	mm	48mm	Inner diameter of the rotor core
Length	\$Lstack	mm	110mm	Length of the rotor core
Steel Type	NLMK - NV355-145, B-H at 60Hz	–	–	Steel type of the rotor core
Stacking Factor	0.95	–	0.95	Stacking factor of the rotor core
Number of Poles	8	–	8	Number of poles of the rotor core
Embrace	\$g_br	–	0.49	Pole embrace
Yoke Thickness	\$Wry	mm	32.816319mm	Yoke thickness of the rotor core

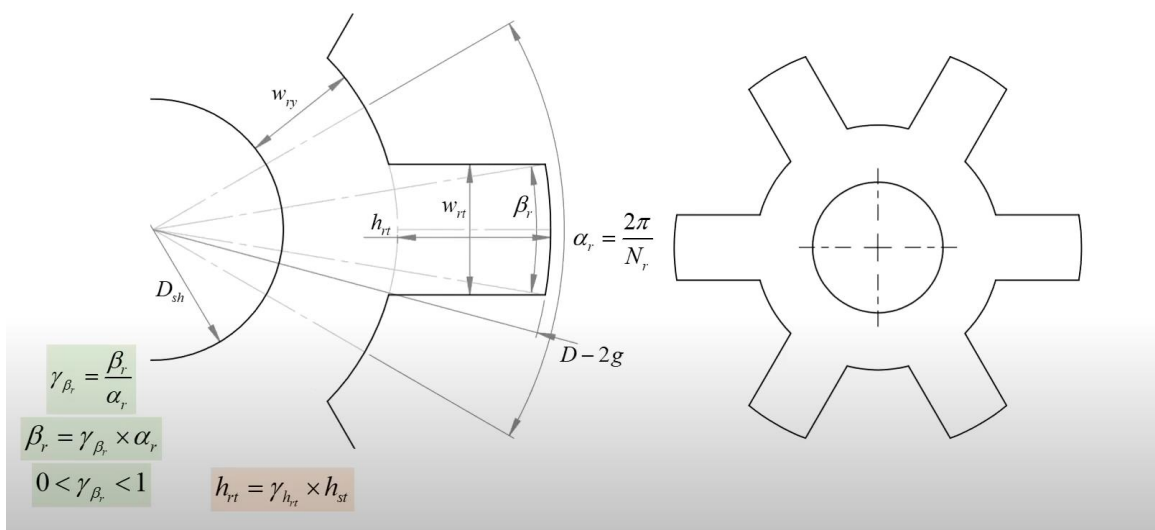


Figure 3 Rotor Lamination Geometry

5.2.3 Circuit and Winding parameters

In the design and simulation of electrical machines, especially motors and generators, accurate input of circuit and winding parameters is crucial for ensuring reliable performance predictions and efficient operation. This section presents the key circuit and winding parameters used in the simulation model.

a) Circuit Parameters

The circuit parameters define the electrical characteristics of the switching and conduction circuitry involved in the power conversion system. These parameters influence the timing, switching behaviour, and voltage losses in the power electronics interface. The parameters used are as follows:

- Lead Angle: The lead angle is set to 22.5 degrees. It indicates the electrical angle by which the triggering signal leads the rotor position in the simulation. This helps in improving motor torque and efficiency at higher speeds by advancing the commutation.
- Trigger Pulse Width: Defined as 156.5 degrees, this parameter specifies the duration for which the gate signal is applied to trigger the switching devices (such as transistors or IGBTs) in electrical degrees.
- Transistor Drop: This is the voltage drop across a single transistor when it is in the conducting state. The value is set to 0.8 V, which represents the loss occurring during conduction and impacts the overall system efficiency.
- Diode Drop: The voltage drop across a single diode during forward conduction is 0.7 V, which is typical for standard silicon diodes. This value is important for calculating total losses in the freewheeling and rectifying circuits.

These parameters are essential to model the non-ideal behaviour of semiconductor components in a real-world circuit.

Table 5Circuit Parameters

Name	Value	Unit	Evaluated Value	Description
Lead Angle of Trigger	22.5	deg	22.5deg	Lead angle of trigger in electrical degrees
Trigger Pulse Width	156.5	deg	156.5deg	Trigger pulse width in electrical degrees
Transistor Drop	0.8	V	0.8V	Voltage drop of one transistor
Diode Drop	0.7	V	0.7V	Voltage drop of one diode

b) Winding Parameters

The winding parameters describe the physical and electrical configuration of the motor windings. These values directly affect the magnetic field generation, copper losses, and the thermal profile of the machine. The defined parameters are as follows:

- Insulation Thickness: Set to 0.02 mm, it represents the thickness of the insulation material wrapped around each conductor strand, which ensures electrical isolation between turns.
- End Adjustment: Given as 10 mm, it accounts for the physical extension of winding ends beyond the core (typically on one side) for making external electrical connections.
- Parallel Branches: Set to 2, this indicates the number of parallel paths through which current can flow within a single phase winding. More branches can reduce resistance and heat generation.
- Turns per Pole: Defined as 16, it indicates the number of wire turns around each pole of the stator. This impacts the magnetic flux and induced EMF in the motor.
- Number of Strands: The value is 1, meaning the winding is composed of a single conductor strand per turn. In some cases, multiple strands (litz wire) are used to reduce skin effect.

- Wire Wrap: Set to 1 mm, this represents the double-side wrapping or mechanical insulation layer over the wire bundle, which protects the windings and helps in mechanical stability.
- Wire Size: The wire used has a diameter of 2.588 mm, which significantly affects current-carrying capacity and resistance. Larger diameters allow higher current flow with lower losses but are harder to wind.

These parameters are fundamental in determining the machine's electromagnetic behaviour, thermal characteristics, and overall performance.

Table 6 Winding parameters

Name	Value	Unit	Evaluated Value	Description
Insulation Thickness	0.02	mm	–	Thickness of the insulation
End Adjustment	10	mm	–	One-side end extension
Parallel Branches	2	–	–	Number of parallel branches
Turns per Pole	16	–	16	Number of turns per pole
Number of Strands	1	–	1	Number of strands per conductor
Wire Wrap	1	–	1	Double-side wire wrap turns
Wire Size (Diameter)	2.588	mm	–	Wire size (diameter)

5.2.4 Conditions on Arc Angles

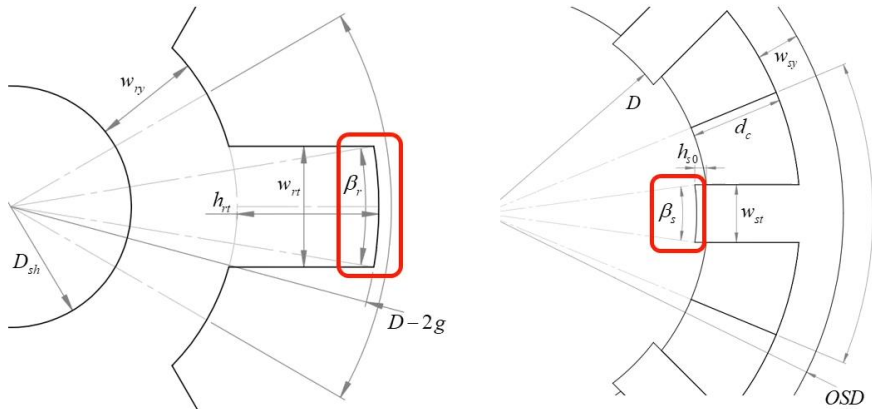


Figure 4Arc Angle Conditions

Conditions on Selection of Arc Angles

- Self-starting requirements (Starting Torque)
- Shaping of static torque vs. rotor position characteristics to have a good performance
- Avoiding negative torque generation

To achieve **self-starting**, smooth **static torque**, and **avoid negative torque**, the following conditions must be satisfied:

Design Constraints

1. Self-Starting Condition:

$$\beta_r < \beta_s$$

Ensures there's no dead zone in the torque vs. position curve at standstill.

2. No Overlap Between Two Stator Poles:

$$\beta_s + \beta_r < \alpha_s$$

Where α_s is the stator pole pitch:

$$\alpha_s = 2\pi/N_s$$

3. **Good Torque Profile:** Adjust $\gamma_{ps} = \beta_s/\alpha_s$ and $\gamma_{pr} = \beta_r/\alpha_r$ within:

$$0.45 < \gamma_{ps} = < 0.5 \text{ and } 0.45 < \gamma_{pr} < 0.5$$

Rotor Pole Arc Angle

$$\beta_r = \gamma_{pr} \cdot \alpha_r = 0.49 \cdot \frac{2\pi}{8} = 0.49 \cdot 0.7854 = [0.3848 \text{ rad} \approx 22.04^\circ]$$

Stator Pole Arc Angle

$$\alpha_s = \frac{2\pi}{N_s} = \frac{2\pi}{12} = 0.5236 \text{ rad} \approx 30^\circ$$

Assuming similar stator pole embrace:

$$\gamma_{ps} \approx 0.45 \Rightarrow \beta_s = \gamma_{ps} \cdot \alpha_s = 0.45 \cdot 0.5236 = [0.2356 \text{ rad} \approx 13.5^\circ]$$

5.2.5 Circuit Design

a) Overview

The circuit represents a three-phase inverter-based motor drive system. It utilizes six switching devices (likely IGBTs or MOSFETs) arranged in a three-phase bridge topology, combined with flyback diodes for freewheeling current management. Each phase (A, B, and C) is equipped with resistive and inductive components that mimic the characteristics of a real three-phase load, typically an electric motor. The design supports current and voltage measurements for control and analysis purposes.

b) Three-Phase Load Modelling

Each of the three phases—A, B, and C—consists of the following:

- Series Resistance (RA, RB, RC):
 - Value: 0.0213293 Ω
 - Purpose: Models the copper losses and inherent resistance of the windings in the load or motor.
- Series Inductance (LA, LB, LC):
 - Value: $4.66028 \times 10^{-6} H \times Kle$
 - Purpose: Represents the inductance of each motor phase. The multiplication factor "Kle" likely represents a scaling or configuration coefficient that adjusts inductance based on design parameters.

These R-L branches accurately emulate the electromagnetic and thermal characteristics of real motor windings under inverter control.

c) Voltage Measurement Points

- Voltage Labels (VIA, VIB, VIC):
These are voltage measurement probes placed at the terminals of phases A, B, and C, respectively, to monitor the output phase voltages from the inverter.
- DC Voltage Sources:
 - Labels: V98+, V105+, V112
 - Each source provides 1V, indicating a simplified or symbolic representation for simulation; in a practical system, this would be replaced by a high-voltage DC link (e.g., 400V or 800V) derived from rectified AC mains or a battery pack.

d) Resistive Load Branches

- Resistors (R119, R126, R133):
 - Value: $100\ \Omega$ each
 - These are connected in parallel or series paths, possibly representing a braking resistor or additional load for each phase, or functioning as current sensors.

e) Current Measurement Blocks

- Labels (IVc1, IVc2, IVc3):
 - These blocks are positioned in each phase and are used to measure current flowing through phases A, B, and C.
 - Essential for feedback in control algorithms such as Field-Oriented Control (FOC) or Direct Torque Control (DTC).

f) DC Link Voltage Sources

- Label IDs: V161 and V168

- Both sources provide 220V, simulating the DC supply provided to the inverter. This is representative of the high-voltage bus feeding the inverter bridge.

g) Power Switches and Diodes

- Switches (S_259 to S_294):
 - These are six semiconductor switches forming a standard three-phase inverter bridge.
 - They operate in pairs to produce PWM-controlled AC output across the three phases.
 - Likely controlled by an external PWM controller or SPWM/Space Vector PWM algorithm in a simulation environment.
- Diodes (D175 to D252):
 - These are freewheeling diodes connected in anti-parallel with the switching devices.
 - Purpose: Provide a path for the inductive load current during the switch-off state, preventing voltage spikes due to inductive kickback.

h) Component Models

- DModel1 and SModel1:
 - These model identifiers indicate the use of standardized semiconductor component models in the simulation.
 - DModel1 refers to the diode characteristics, while SModel1 refers to the switching element's behaviour (e.g., IGBT, MOSFET, etc.).

i) Control and Monitoring Considerations

- The circuit includes comprehensive monitoring via voltage and current sensors across each phase, allowing integration with control algorithms for motor control, fault detection, or performance analysis.
- The inverter topology is compatible with various motor types, including induction motors, synchronous machines, or BLDC motors, depending on the control logic applied externally.

j) Application Context

This type of circuit is fundamental in electric drives, such as:

- Electric vehicles (EVs)
- Industrial motor drives
- Renewable energy systems (e.g., solar inverters)
- HVAC systems

Its modularity and detailed parameterization make it suitable for simulation studies on efficiency, harmonic distortion, thermal behaviour, and dynamic response under various operating conditions.

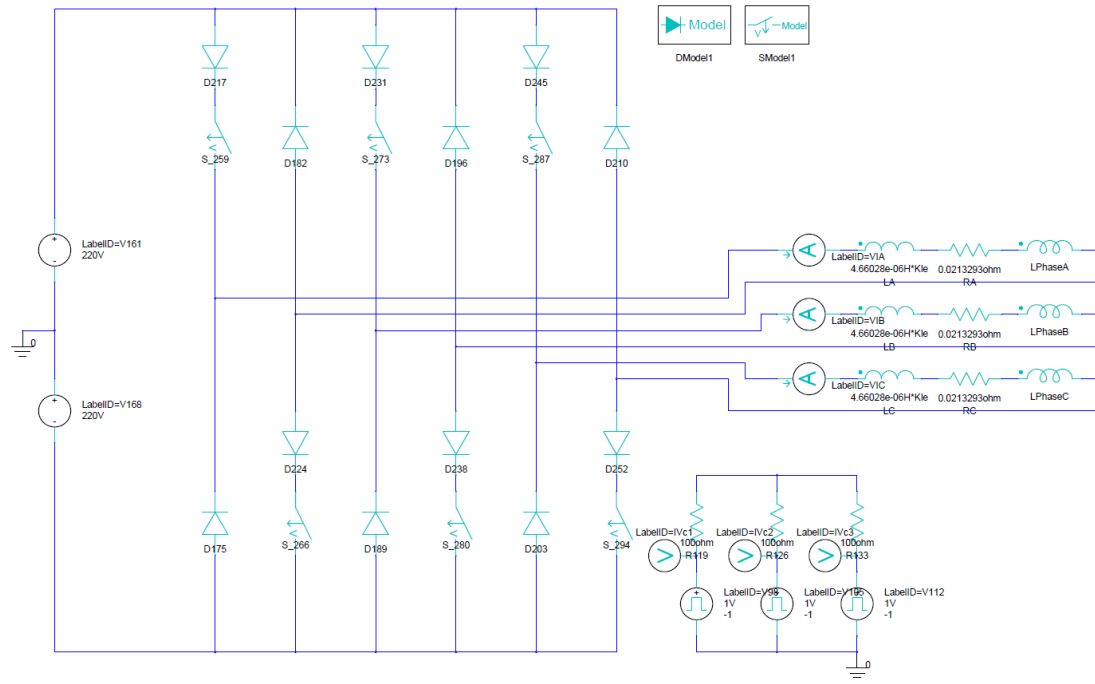


Figure 5Circuit Design

5.3 2-D Geometry and Meshing

Key Geometry Parameters:

- Stator Outer Diameter (Osd) = 250 mm
- Stator Diameter (SD) = 158 mm
- Stator Pole Angle = 30°
- Rotor Pole Angle = 45°
- Slot Opening = 2 mm
- Air Gap = 1 mm
- Stack Length = 110 mm
- Shaft Diameter = 48 mm

- Rotor Tooth Width = 29.83 mm
- Stator Tooth Width = 21.03 mm

Meshing Strategy:

- High mesh density in the airgap and pole regions
- Adaptive refinement used to ensure convergence
- Skewness < 0.7, Mesh Quality > 0.8

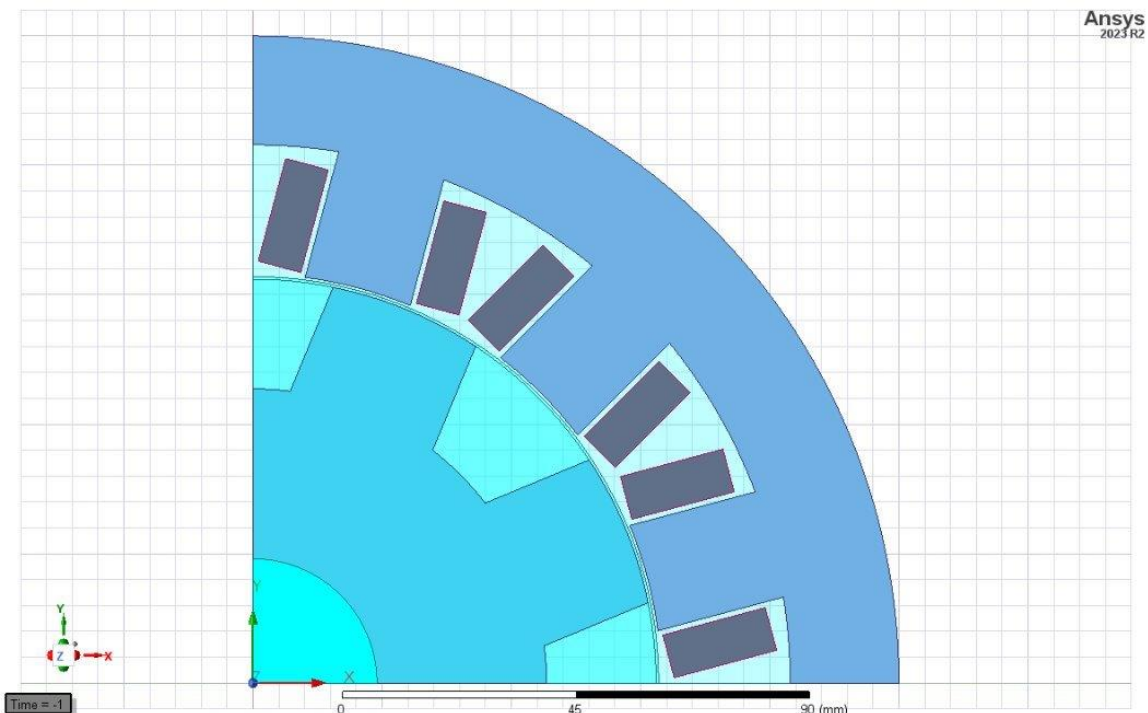


Figure 6 2D Geometry

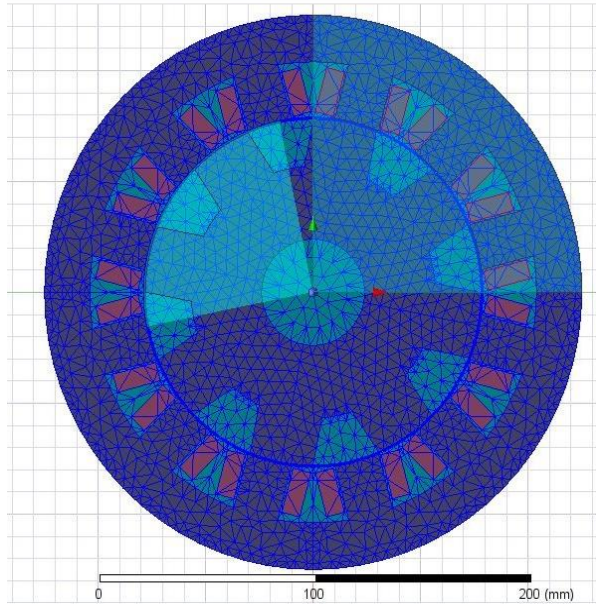


Figure 7 Meshing

5.4 Simulation Output (*MAXWELL 2D*)

This section presents the comprehensive output plots and simulation results obtained using ANSYS Maxwell 2D. It includes details of the simulation setup, key configuration parameters, and resulting performance metrics. The plots illustrate the electromagnetic behaviour of the designed 12/8 switched reluctance motor (SRM) under defined operating conditions. These outputs serve to validate the design choices and provide insights into torque generation, magnetic flux distribution, current waveform behaviour, and overall machine performance.

5.4.1 Flux Linkage vs Current (at Varying Rotor Positions)

Figure 8 represents the variation of flux linkage with respect to stator current across multiple rotor positions in the 12/8 Switched Reluctance Motor (SRM) design. The simulation was conducted in ANSYS Maxwell 2D, and data was post-processed to generate the curves for rotor positions ranging from 0° to 100° electrical, in intervals of 10° or 20° .

Plot Details

- X-Axis: Phase Current (Amperes)
- Y-Axis: Flux Linkage (Weber)
- Multiple Curves: Each curve corresponds to a distinct rotor position, highlighting the magnetic behaviour as the rotor moves from aligned to unaligned position.

Key Observations and Analysis

1. Linear Magnetic Behaviour (0 A to \sim 200 A)

In this region, the flux linkage increases linearly with current across all rotor positions. This indicates that the magnetic material (core) is operating well below its saturation level, and the relationship between current and flux remains predictable and proportional.

This is the optimal operating region for efficiency and minimal losses.

2. Nonlinear Magnetic Behaviour (>200 A)

Beyond \sim 200 A, the curves begin to bend, showing a nonlinear increase in flux linkage. This is a clear indication of magnetic saturation in the iron core.

- At this point, even a large increase in current produces only a marginal increase in flux linkage.
- This reflects the saturation limits of the stator/rotor teeth.

3. Rotor Position Dependence

- Higher Flux Linkage at 0° and 20° : These positions correspond to aligned conditions, where stator and rotor poles are magnetically aligned, yielding maximum inductance and flux linkage.
- Lower Flux Linkage at 80° and 100° : These correspond to unaligned positions, where inductance is minimum due to greater magnetic reluctance between stator and rotor poles.
- The spacing between the curves decreases in saturated regions, indicating that rotor position has less influence on flux linkage when saturation dominates.

Significance in SRM Design

- This plot is fundamental for nonlinear modelling of the SRM, especially in control algorithms like torque sharing and current profiling.
- The hysteresis and saturation characteristics inferred from this curve are crucial for:
 - Accurately calculating instantaneous torque
 - Predicting flux weakening behaviour at high speeds
 - Implementing optimal excitation strategies

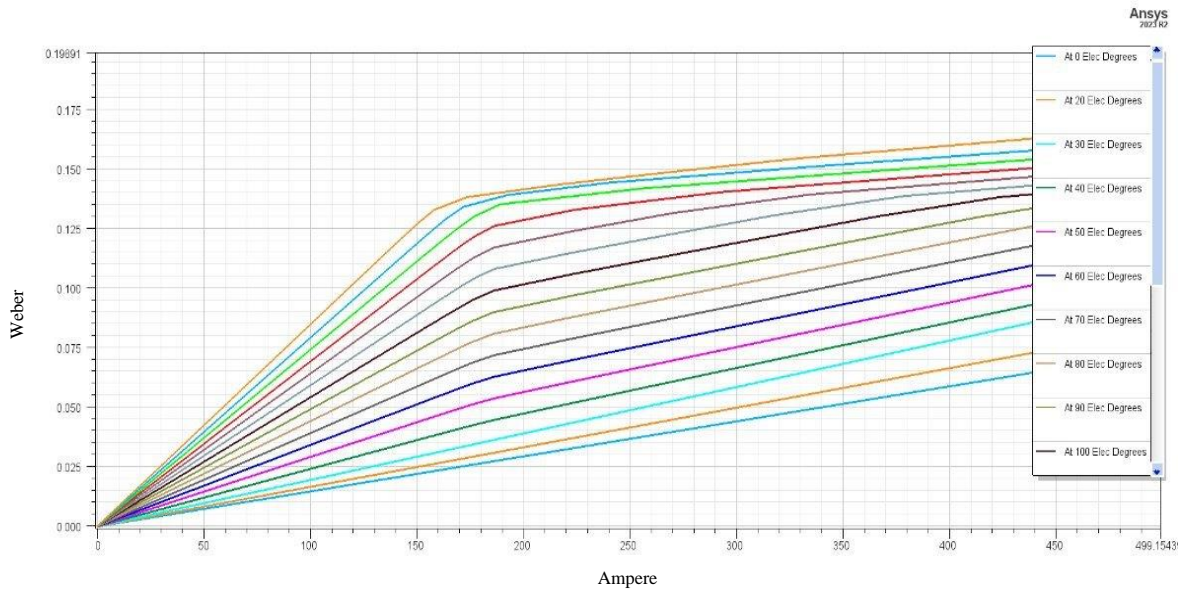


Figure 8 Flux Linkage Vs Current (at Varying Rotor Positions)

5.4.2 Efficiency vs Speed (SRM 12/8)

In Figure 9, the efficiency characteristics of the designed SRM were analysed across a wide speed range (0 to 8000 RPM), under standard operating conditions. The following detailed observations highlight how the motor transitions from inefficient to highly efficient operation as speed increases.

- ◆ Low Efficiency at Low Speeds (0–2000 RPM)

At start-up and low-speed conditions, the motor experiences a significant drop in efficiency, typically below 70%. This behaviour is attributed to the following key factors:

- High Input Current Demand:

At low speeds, the motor's back-EMF is negligible, leading the controller to inject higher current to generate the required starting torque. This elevated current contributes to:

- Increased copper losses (I^2R) in the windings
 - Potential localized heating in the stator coils
 - Low Mechanical Output Power:
Mechanical power ($P = \text{Torque} \times \text{Speed}$) remains low due to the low rotational speed, even if torque is maintained. As a result:
 - The input power remains high, but
 - The output power is minimal, resulting in poor efficiency.
 - Switching Losses Dominate:
At low speeds, the SRM operates at higher switching frequencies with smaller dwell angles, adding to switching and core losses.
- ◆ Rapid Efficiency Increase (2000–5000 RPM)

In this mid-speed range, the motor shows a rapid improvement in efficiency, often rising above 80%. This transition is driven by:

- Back-EMF Contribution:
As speed increases, back electromotive force (EMF) rises proportionally, aiding in the natural development of torque with lower current injection, thereby reducing copper losses.
- Improved Energy Conversion:
The motor reaches an optimal torque-generation zone where:
 - The energy supplied is more efficiently converted to mechanical output
 - Losses are comparatively minimized

- Magnetization and Demagnetization Control Improve:

At these speeds, current chopping and control strategies (like turn-on/turn-off angles) operate in more stable regions, reducing flux overshoots and hysteresis effects.

- ◆ Efficiency Peaks at High Speeds (6000+ RPM)

In this zone, the SRM reaches its optimal performance, with efficiency consistently exceeding 90%, as designed for high-speed EV applications. The following effects dominate:

- Reduced Conduction Losses:

Due to rising back-EMF, the required phase current further decreases, leading to minimal copper losses.

- Lower Switching and Iron Losses:

At higher speeds, longer dwell times and less aggressive PWM switching reduce dynamic losses in power electronics and stator laminations.

- Stable Magnetic Behaviour:

The rotor operates in a quasi-steady state where the magnetic cycles are smooth, minimizing hysteresis and eddy current losses.

- Mechanical Power Maximization:

As torque is moderately sustained and speed is maximized, mechanical power output reaches its peak, which boosts efficiency.

Design Implication

The simulation confirms that the 12/8 SRM design is optimized for high-speed operation, making it ideal for EV/HEV propulsion, where high efficiency at cruising speeds (6000–8000 RPM) is critical for extending vehicle range and reducing thermal stress on the motor and converter.

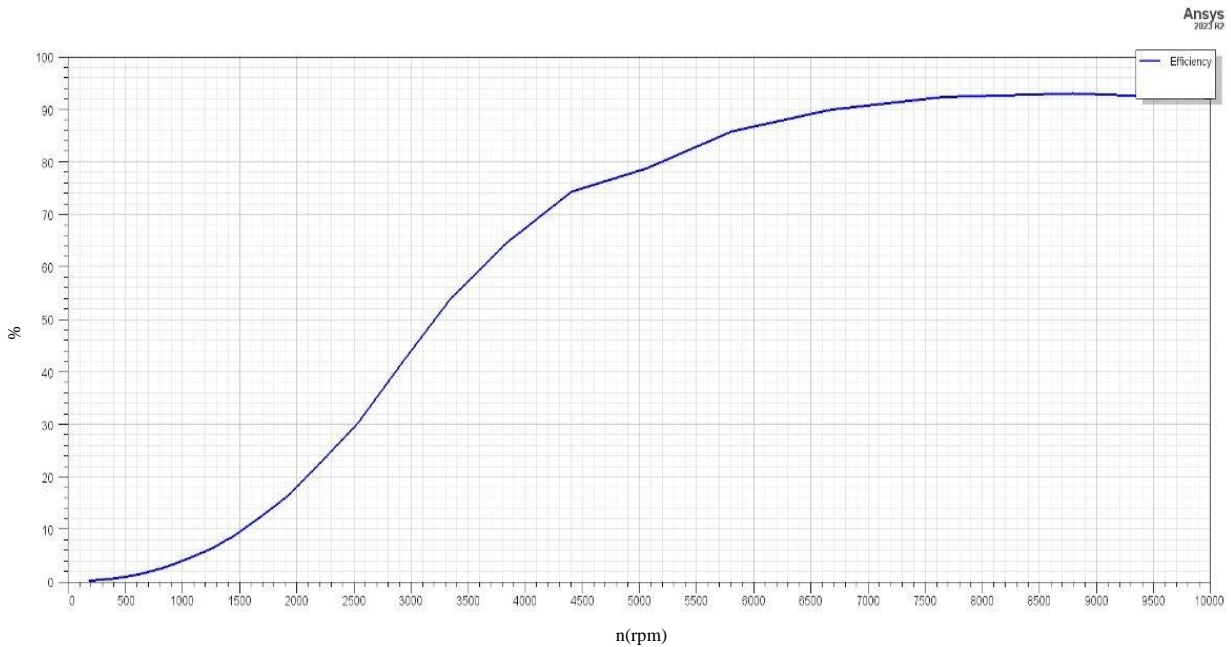


Figure 9 Efficiency Vs Speed

5.4.3 Output Power Vs Speed

Figure 10 illustrates the **variation of mechanical output power** as a function of motor speed (RPM) under rated voltage and optimized firing angles. It provides crucial insight into the **torque-speed-power trade-off** inherent to Switched Reluctance Motors (SRMs), especially in traction applications.

- ◆ Initial Power Rise (0–3500 RPM)

In this low-to-mid-speed zone, the SRM shows a progressive increase in output power, characterized by:

- Increasing Torque Generation:

At lower speeds, the torque output is high due to effective current injection and strong magnetic attraction between stator and rotor poles.

- Higher Current Availability:

Since back-EMF is low in this range, the power converter easily drives high current into the windings. This leads to:

- Higher magnetic field strength
- Stronger electromagnetic interactions

- Efficient energy conversion into rotational motion
- Mechanical Power ($P = T \times \omega$) Increases:
As the speed (ω) increases, the mechanical output rises proportionally, even if torque begins to slightly decline due to iron saturation or control limits.

◆ Peak Power Zone (~3500–4000 RPM)

At this operating point, the motor reaches its maximum power output, around 170 kW, representing the peak operating efficiency and performance of the design:

- Torque-Speed Product is Maximized:
While torque may begin to decline slightly due to increased back-EMF, the high rotational speed compensates, resulting in peak power.
- Back-EMF and Current Are Balanced:
This range represents a sweet spot where:
 - Back-EMF aids smooth operation but hasn't yet started to choke current flow significantly.
 - The controller still manages to maintain strong phase excitation.
- Stable Converter Operation:
The power electronics operate under optimal conditions, with manageable switching frequency and voltage stress.

◆ Power Decline Beyond 4000 RPM

As speed further increases, a notable drop in output power is observed, due to multiple high-speed limitations:

- Dominance of Back-EMF:
At high RPM, back-EMF rises substantially, opposing the input voltage and limiting current flow into the stator windings.
- Reduced Effective Torque:
With less current excitation, magnetic pull weakens, and the torque output drops — despite the rising speed, the overall power starts to decline.
- Increased Switching and Iron Losses:
High-frequency switching and rapid magnetic reversals introduce:

- Greater core (hysteresis + eddy current) losses
- Switching losses in MOSFETs/IGBTs due to higher dV/dt and dI/dt
- Thermal Constraints:
At high power densities, thermal rise in the stator and converter can further throttle current injection via thermal derating or controller protection logic.

Design Relevance

This power profile confirms the motor is optimized for traction scenarios, delivering high power (~170 kW) in the medium-speed region suitable for vehicle acceleration, while maintaining acceptable performance in cruising speeds (6000–8000 RPM), where power is no longer peak but efficiency is highest.

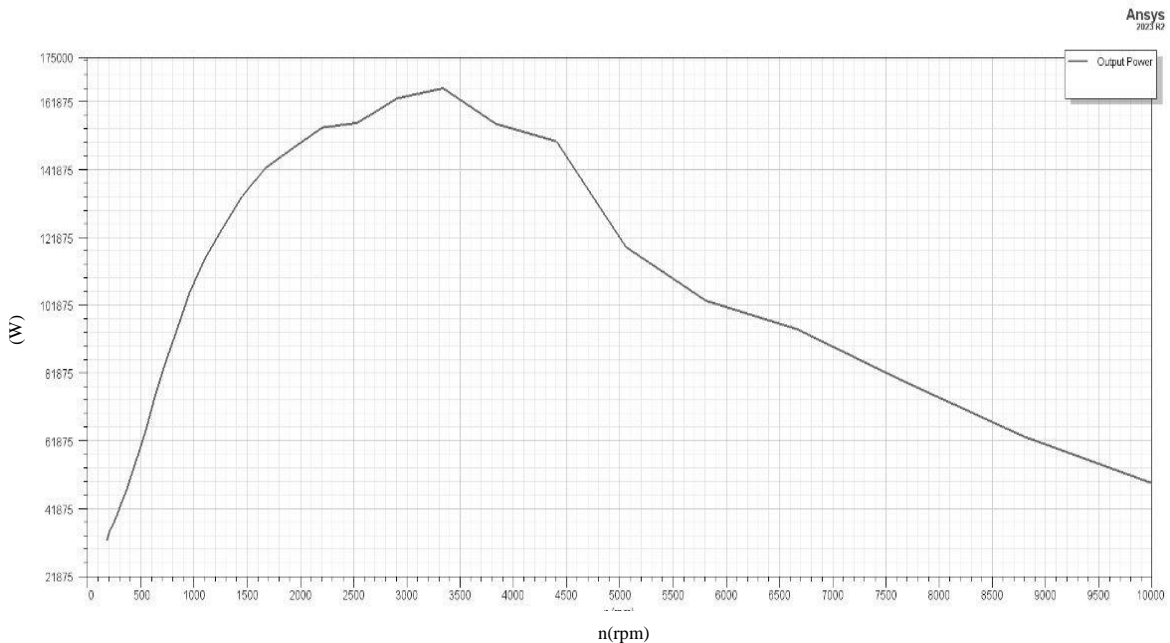


Figure 10 Output Power Vs Speed

5.4.4 Torque Vs Speed

Figure 11 illustrates how the developed electromagnetic torque of the SRM varies with motor speed (RPM). The curve showcases the typical behaviour of a switched reluctance machine optimized for high torque at low speeds and efficient operation across a wide range.

- ◆ High Torque at Low Speeds (0–500 RPM)

- Starting Torque Peaks Around 1700 Nm:

At standstill and very low speeds, the SRM exhibits extremely high torque output, which is essential for:

- Initial acceleration of EVs
 - Hill starts and heavy-load conditions

- Why Torque Is High:

- At zero or low back-EMF, maximum current can be applied without significant opposition.
 - Strong magnetic alignment between stator and rotor poles allows full utilization of magnetic reluctance force.
 - The rotor remains in the high inductance region for longer, enhancing torque build-up.

- This Region Shows the SRM's Strength:

The high pull-out torque at low RPMs is a key advantage of SRMs in traction systems.

- ◆ Gradual Torque Decline (500–4000 RPM)

- Torque Drops from ~1200 Nm to ~400 Nm:

As speed increases, torque gradually declines. This is a result of:

- Rising back-EMF, which resists phase current injection
 - Reduced dwell time of current excitation due to shorter conduction periods at higher speeds
- Impact of Control Strategy:

Even though dwell angle and firing position are optimized, the reduced phase overlap at higher RPM leads to:

 - Shorter torque-producing intervals
 - Lower net average torque per cycle
 - Why This Range Is Still Efficient:

Despite lower torque, the increase in speed compensates for output power (as $P = T \times \omega$), leading to the peak power zone around 4000 RPM.
- ◆ Significant Torque Drop Beyond 4000 RPM
 - Torque Falls Below 100 Nm by 8000 RPM:

This steep fall-off highlights the upper limit of the motor's speed capability in torque production.
 - Key Reasons for Drop:
 - Back-EMF >> Supply Voltage, choking current flow
 - Insufficient magnetic pull due to minimal current injection
 - Limited excitation window as speed increases and electrical degrees pass too quickly
 - Higher switching and core losses reduce usable magnetic energy
 - Implications for Vehicle Application:

- At very high RPMs, the motor enters a cruising mode where torque is no longer used for acceleration but for maintaining motion.
- Vehicle operation must shift to gear-assisted control or field weakening strategies if more torque is needed.

Relevance

This torque-speed curve confirms the SRM's suitability for traction systems:

- Strong low-speed torque for vehicle launch
- Moderate torque in mid-speed range enabling peak power
- Low torque at high RPM, requiring smart control strategies or supporting gearboxes

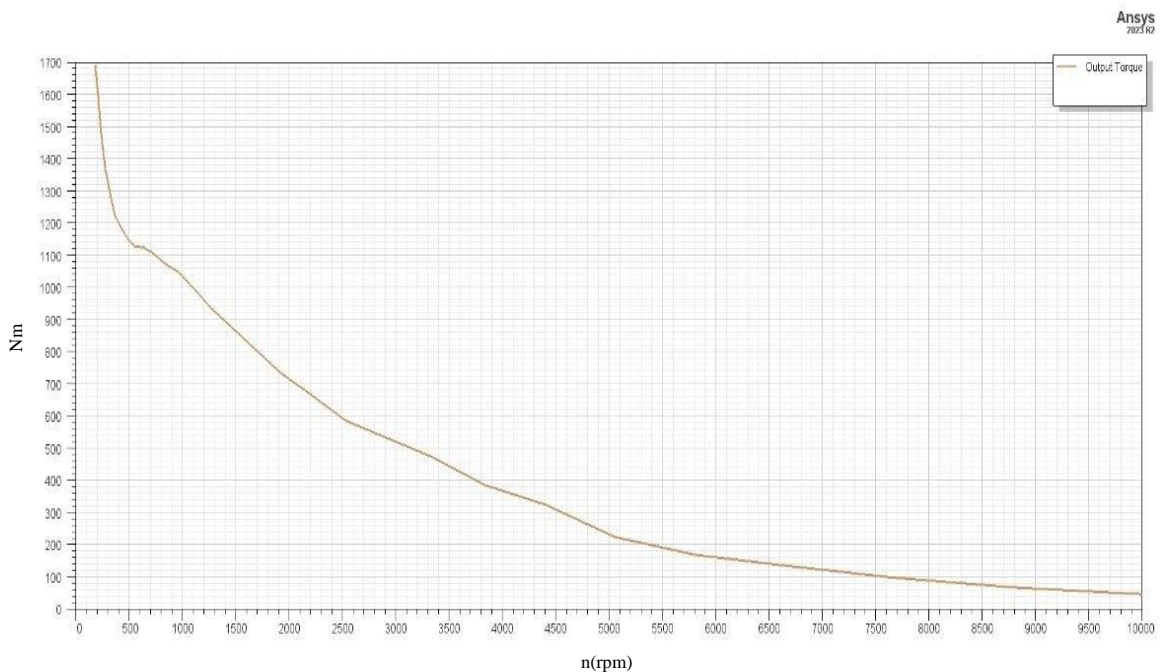


Figure 11 Torque Vs Speed

5.4.5 Rated Phase Current Vs Electric Degree

Figure 12 shows the phase current waveform across one electrical cycle. The waveform is crucial for analysing current control, excitation timing, and energy conversion behaviour of switched reluctance motor.

- ◆ 1. Peak Phase Current $\approx 550\text{--}600\text{ A}$

- Sharp Ramps and Peaks:

The phase current rises rapidly when the rotor enters the aligned inductance region, peaking at about 120° and 480° electrical.

- Significance of High Peak:

- High current = strong magnetic field in stator = greater electromagnetic torque (as we saw in the torque-speed plot).
 - This confirms SRM is designed for high starting torque and rapid acceleration.

- Consistent with Low-Speed Performance:

At low speeds, lower back-EMF allows such high currents to be injected, directly supporting the observed 1700 Nm starting torque.

- ◆ 2. Pulse Shape – Asymmetric and Typical of SRM Behaviour

- Asymmetric Rise and Fall Edges:

The rising edge of the current is sharper than the falling edge, due to:

- Fast current injection at the start of excitation
 - Slower current decay after the rotor passes the aligned position

- Linked to Trigger Pulse Width (156.5°):

- The current profile matches a single-pulse excitation strategy
 - Wide triggering pulse allows longer conduction time, giving the current more time to build up and decay

- Control Strategy Insight:

This waveform supports a non-overlapping, sequential phase excitation—simplifying control but also ensuring clean phase operation.

- ◆ 3. Flat-Bottomed Zero-Current Zone

- Long Duration of Zero Current Between Pulses:

The waveform stays flat at zero current for a significant portion of the electrical cycle between 180° – 480° and 540° – 960° .

- Implications:

- No overlap between consecutive phase conduction → prevents mutual magnetic interference
 - But it also means lower average torque per cycle, since only one phase contributes torque at a time

- Trade-off:

- Ideal for reducing torque ripple and simplifying drive circuitry
 - However, it limits total torque output unless compensated with high peak currents (which this design achieves)

This current waveform confirms this SRM's:

- High torque production at low speed (due to high peak phase current)
- Clean single-pulse conduction strategy, optimized via 156.5° trigger width
- Non-overlapping excitation, minimizing losses and crosstalk between phases

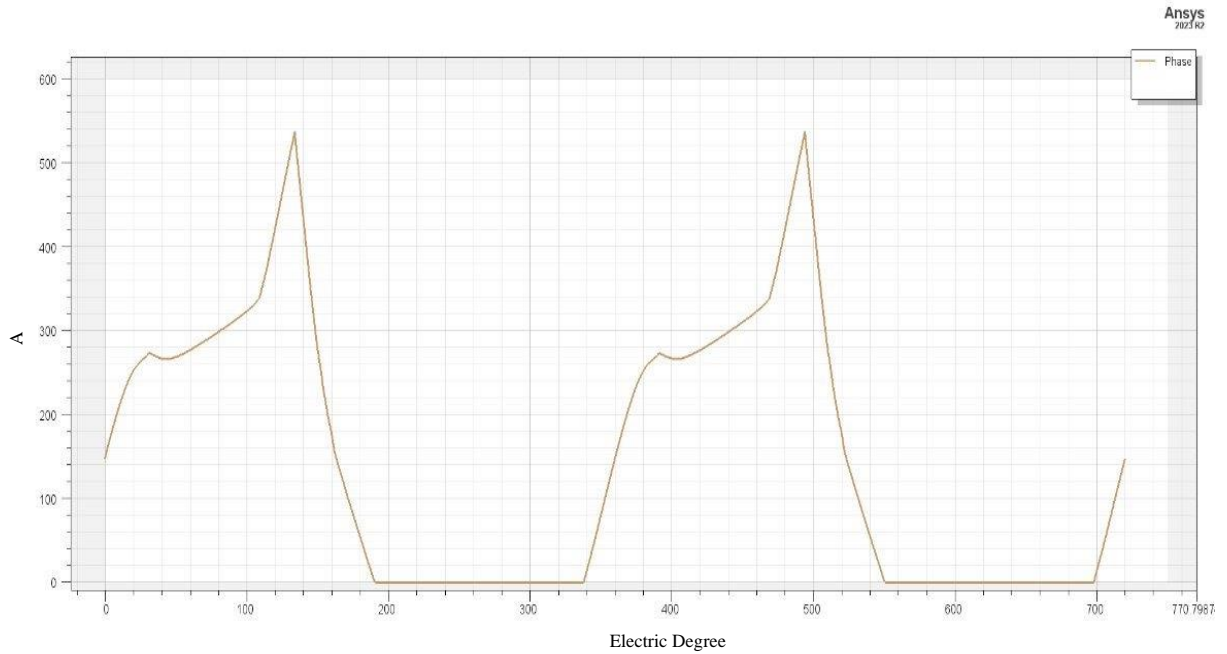


Figure 12 Rated Phase Current Vs Electric Degree

5.4.6 Air gap Inductance

Figure 13 illustrates how the phase inductance changes over an electrical cycle as the rotor moves relative to the stator poles. It provides vital insight into the electromagnetic geometry of 12/8 SRM and its performance in terms of energy conversion.

- ◆ Minimum Inductance – Unaligned Position
 - Positions:
Occurs at approximately 0° , 360° , and 720° electrical.
 - Inductance Value:
Around 0.11 mH, the lowest point in the cycle.
 - Explanation:
 - In these positions, the rotor teeth are completely misaligned with the stator poles.
 - The magnetic path experiences maximum air gap, which increases the reluctance and lowers inductance.

- Minimal flux linkage occurs at this point due to the weak magnetic coupling.
- Significance:
These are ideal positions to turn off the phase current, since the electromagnetic torque generated here is negligible. This supports efficient excitation timing to reduce power losses.

◆ Maximum Inductance – Aligned Position

- Positions:
Peaks are seen at approximately 180° and 540° electrical.
- Inductance Value:
Around 0.9 mH, which is the highest inductance reached during one cycle.
- Explanation:
 - At these points, the rotor poles are perfectly aligned with the stator poles.
 - The magnetic path becomes shortest and least resistive, minimizing magnetic reluctance.
 - This leads to maximum magnetic flux linkage and hence maximum inductance.
- Significance:

These are the optimal points for peak torque production. Energizing the phase around these aligned positions extracts the most torque per ampere of current.

◆ Significance

The inductance profile over an electrical cycle directly affects:

- Torque Production: Torque in an SRM is proportional to the rate of change of inductance with respect to rotor position.
- Trigger Pulse Optimization: The wider the gap between minimum and maximum inductance, the better control range you have for optimizing triggering angles.
- Magnetic Design Validation: Results (0.11 mH to 0.9 mH) show a robust magnetic design, capable of producing strong torque during aligned regions and low losses during unaligned ones.

- The SRM's magnetic behaviour is functioning correctly:
 - Low inductance in unaligned positions (for turn-off)
 - High inductance in aligned positions (for torque production)
- The wide inductance swing (~0.11 to ~0.9 mH) is favourable for efficient and dynamic torque generation.

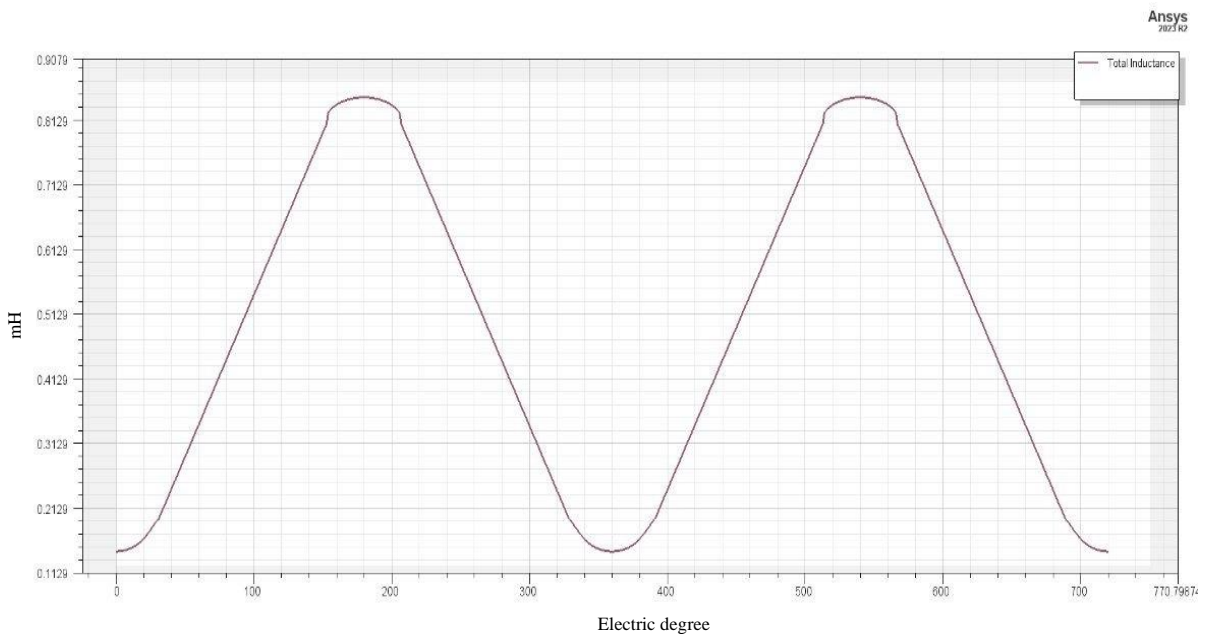


Figure 13 Airgap Inductance Vs Electric Degree

5.4.7 Torque waveform (torque vs time)

Figure 14 shows the instantaneous torque output of the SRM over a short time window. It helps assess both the dynamic behaviour and stability of the motor's electromagnetic torque profile during operation.

- ◆ Torque Range Overview

Table 7 Torque Range Overview

Parameter	Value
Peak Torque	~152 Nm
Trough (Min) Torque	~95–100 Nm
Average Torque	~125 Nm
Torque Ripple	~40–45 Nm (\approx 30–35%)
Firing Interval	~0.3 ms per peak
Cycles Observed	~5.5 cycles in 1.8 ms

- ◆ Key Observations
 - ◆ 1. Initial Ramp-Up
 - The torque waveform smoothly rises from zero after start-up.
 - No high-frequency oscillations or instability are observed during this phase.
 - Indicates that the initial firing sequence and rotor alignment are correctly synchronized.
 - ◆ 2. Periodic Torque Pulses
 - The waveform shows repetitive torque peaks spaced about 0.3 ms apart, which aligns well with the mechanical rotation of an 8-pole rotor.
 - Each peak corresponds to the conduction of one stator pole pair, confirming the correct phase sequence and excitation timing.
 - ◆ 3. Stable Oscillations After Start-Up
 - Once the motor stabilizes, the torque waveform exhibits a clean, periodic shape.
 - The waveform maintains consistent frequency and amplitude, confirming a reliable and synchronized switching scheme using the 156.5° conduction angle.

- ◆ Torque Ripple Analysis

- The peak-to-peak torque ripple is about 30–35%, typical of SRM drives due to:
 - Discrete pole excitation.
 - Pulsed magnetic energy conversion.
- Ripple sources:
 - Unbalanced magnetic pull between rotor-stator pairs.
 - Single-phase excitation at a time (non-overlapping mode).

Ripple Implications:

- While noticeable, this ripple is well within acceptable SRM limits.
- Can be mitigated using:
 - Multi-phase overlapping conduction
 - Current profiling
 - Advanced controller strategies (e.g., predictive or adaptive control)
- The SRM demonstrates strong average torque (125 Nm) with high instantaneous peaks (~152 Nm).
- The motor's periodic, stable torque output confirms that:
 - Trigger angle (156.5°) and pulse width are well-chosen.
 - Switching synchronization and conduction intervals are optimized for high performance.
- While ripple exists, the waveform reflects healthy SRM behaviour, suitable for EV drive cycles where torque ripple can be filtered by mechanical inertia or suspension design.

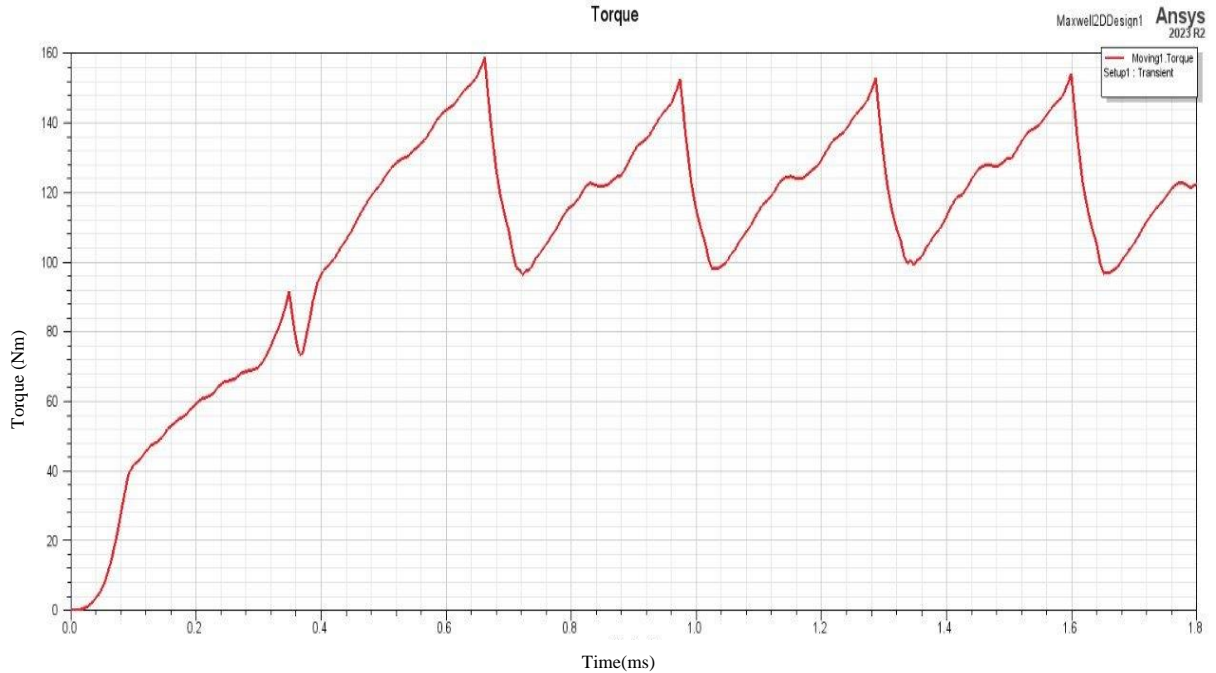


Figure 14 Torque vs Time

5.4.8 Three phase Current vs Time

In Figure 15, the simulation results for the phase currents, identified as Phase A (Red), Phase B (Green), and Phase C (Blue), demonstrate the expected current profiles during operation. Each phase is excited sequentially, with current peaking around 1.1 kA. The current pulse in each phase exhibits a characteristic sharp rise to its peak value, followed by a decay, which aligns with the behaviour expected from an asymmetric converter control strategy.

Key Observations:

- Sequential Phase Excitation:

The phase currents do not exhibit significant overlap, which indicates that the commutation sequence is appropriately spaced. This suggests that the excitation timing matches the 12/8 geometry of the switched reluctance motor, ensuring smooth phase transitions and avoiding potential issues such as torque ripple due to misaligned commutation.

- Peak Current:

A peak current of approximately 1.1 kA is observed during each pulse, which is

consistent with the motor's torque requirements. This value is sufficient for generating the target torque of 150 Nm, and it falls within the practical current limits for high-performance switched reluctance motors used in electric vehicles (EVs). This further supports the feasibility of the motor's design and performance under high-load conditions.

- **Asymmetric Current Profile:**

The current pulse shows a gradual rise at the beginning of the phase, followed by a steep decay. This asymmetric profile is typical for control strategies using chopper circuits. The gradual rise in current occurs during the turn-on phase, where the converter slowly ramps up the current to the motor. The sharp fall during the turn-off phase is indicative of a freewheeling or negative voltage application, which allows for quick current decay, improving efficiency and controlling the motor's speed.

- **Dwell Time (Pulse Width):**

The duration for which each phase remains energized, or the dwell time, is approximately 0.45 ms. This timing aligns with the previously determined 156.5° conduction angle, which matches the motor's operating condition at 8000 RPM. The pulse width of 0.45 ms ensures that each phase remains on for the required duration, optimizing torque generation and motor efficiency.

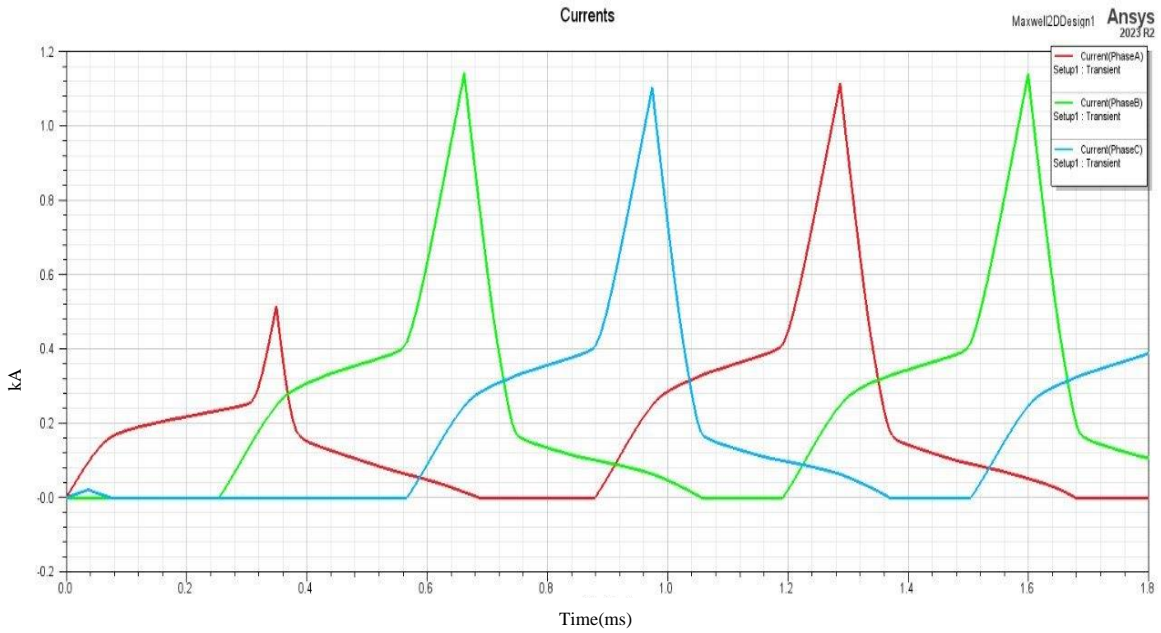


Figure 15 Phase current Vs time

5.4.9 Induced Voltage Vs Time

The induced voltage waveforms in the switched reluctance motor (SRM) exhibit a trapezoidal shape, with distinct flat tops and steep transitions. This characteristic voltage profile is typical for SRMs, which operate with non-sinusoidal back electromotive force (back-EMF). The flat tops indicate periods of constant induced voltage during phase conduction, while the steep transitions correspond to the rapid changes in the magnetic field when the phase is either turning on or off.

- Peak Voltages and Bus Voltage Alignment:

The peak induced voltages in the system approach ± 460 V, which closely matches the DC bus voltage range of 440–480 V used in the system. This alignment confirms that the voltage levels generated by the motor are well within the operational range of the power electronics and the bus voltage, ensuring that the system operates effectively and avoids potential over-voltage conditions. The induced voltage being slightly less than the bus voltage is typical for SRMs,

where the motor voltage is influenced by the rate of change of the magnetic flux during operation.

- **Zero Voltage during De-energized Phases:**

When a phase is not energized, the induced voltage drops to zero, as expected. In the absence of current flow through the phase windings, there is no electromagnetic interaction to generate a voltage, which is characteristic of SRM operation during non-energized phases. This zero voltage state helps to reduce energy consumption during these periods and contributes to the efficiency of the motor.

- **Large Negative Voltage during Turn-Off (Energy Return Phase):**

When the phase is de-energized, a large negative voltage is observed. This negative voltage is a result of the back-EMF generated during the motor's demagnetization process. As the motor rotor moves and the magnetic field collapses, the energy stored in the magnetic field is returned to the DC bus. This return of energy is typical for SRMs, and it helps in regenerating power, reducing overall energy consumption, and improving the system's efficiency. The negative voltage is indicative of the phase current freewheeling in a way that recovers energy rather than dissipating it, which is beneficial for regenerative braking in electric vehicle applications.

- **Timing and Symmetry Between Phases:**

The timing between the three phases is very precise and symmetrical. Each phase transitions from energization to de-energization in a well-coordinated manner, leading to smooth electrical rotation. The smoothness of the voltage transitions between the phases ensures minimal torque ripple and optimized motor performance. This symmetry also indicates that the commutation and phase switching are well-tuned to the motor's mechanical rotation, promoting efficient energy conversion and consistent motor operation. The clean symmetry between phases is vital for achieving smooth and reliable rotation, essential for high-performance electric vehicle applications.

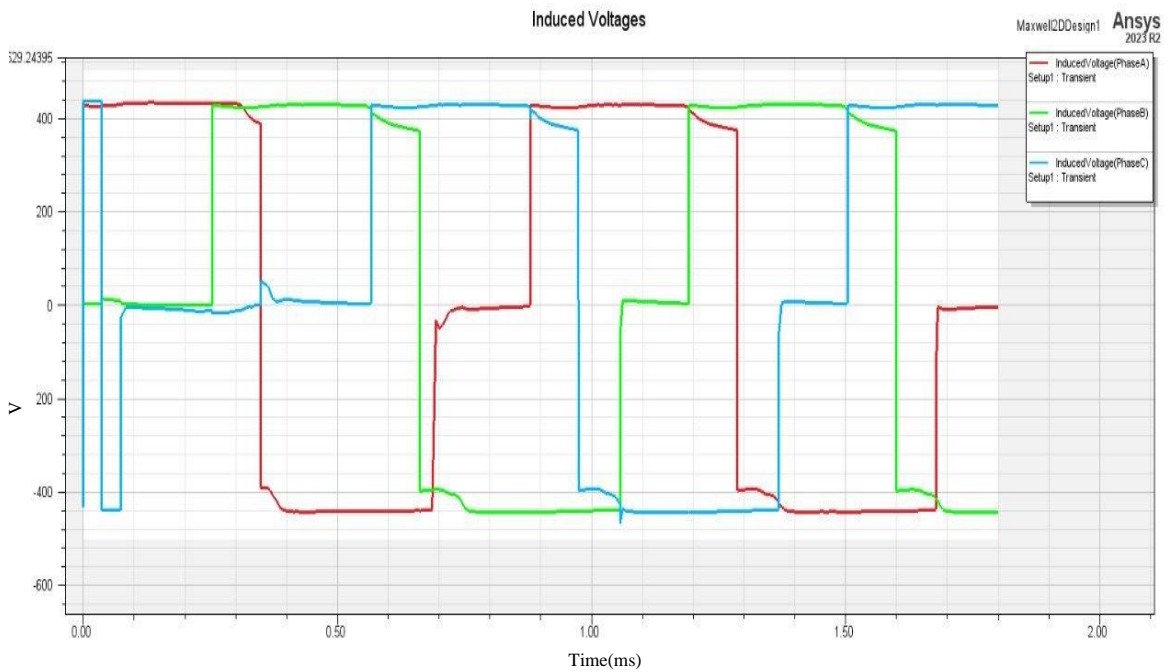


Figure 16 Induced Voltage Vs Time

5.4.10 Flux Linkage Analysis

The flux linkage waveforms (Figure 17) for Phases A, B, and C exhibit high symmetry, strong linearity, and minimal inter-phase coupling, which are indicative of a well-designed switched reluctance motor (SRM) under ideal switching conditions and proper magnetization. These characteristics play a critical role in the motor's performance, contributing to reduced losses and improved efficiency.

Physical Interpretation

- Linear Flux Linkage during Phase Excitation:

The flux linkage for each phase shows a linear rise and fall, which is a direct consequence of the constant voltage applied during phase excitation. This linear behaviour is consistent with the expected back electromotive force (back-EMF) waveform discussed earlier. During phase energization, the flux linkage increases

at a constant rate, reflecting a stable and controlled voltage application. The linearity of this relationship confirms that the motor is operating efficiently, without excessive magnetic saturation or leakage, which would otherwise distort the flux waveform.

- **Minimal Mutual Interference Between Phases:**

Each phase demonstrates minimal mutual interference, meaning the flux linkage of one phase does not significantly affect the others. This is a key benefit of the 12/8 SRM topology, where the magnetic paths of each phase are decoupled. In a well-designed SRM, this lack of cross-coupling ensures that each phase operates independently, allowing for precise control of phase currents and minimizing torque ripple. The absence of significant mutual coupling reduces energy losses and enhances the efficiency of the motor.

- **Clean Flux Transitions and Distinct Rise/Fall:**

The transitions in flux linkage—both during the rise and fall of the waveform—are sharp and distinct, indicating that the motor's magnetic field is transitioning efficiently between phases. These clean transitions are crucial for minimizing torque ripple, which can be detrimental to motor performance, especially in electric vehicle (EV) applications where smooth and consistent torque delivery is required. The ability to achieve such clean flux transitions directly contributes to the motor's overall efficiency by ensuring that energy is transferred without unnecessary fluctuations or losses.

The flux linkage analysis confirms that the 12/8 SRM is operating efficiently, with minimal inter-phase coupling and linear flux dynamics. These attributes are essential for achieving low torque ripple, stable performance, and high efficiency—characteristics that are particularly valuable for high-performance EV applications. The clean flux transitions and decoupled magnetic paths further demonstrate that the motor design is well-optimized for practical use, providing a reliable and robust solution for electric vehicle propulsion.

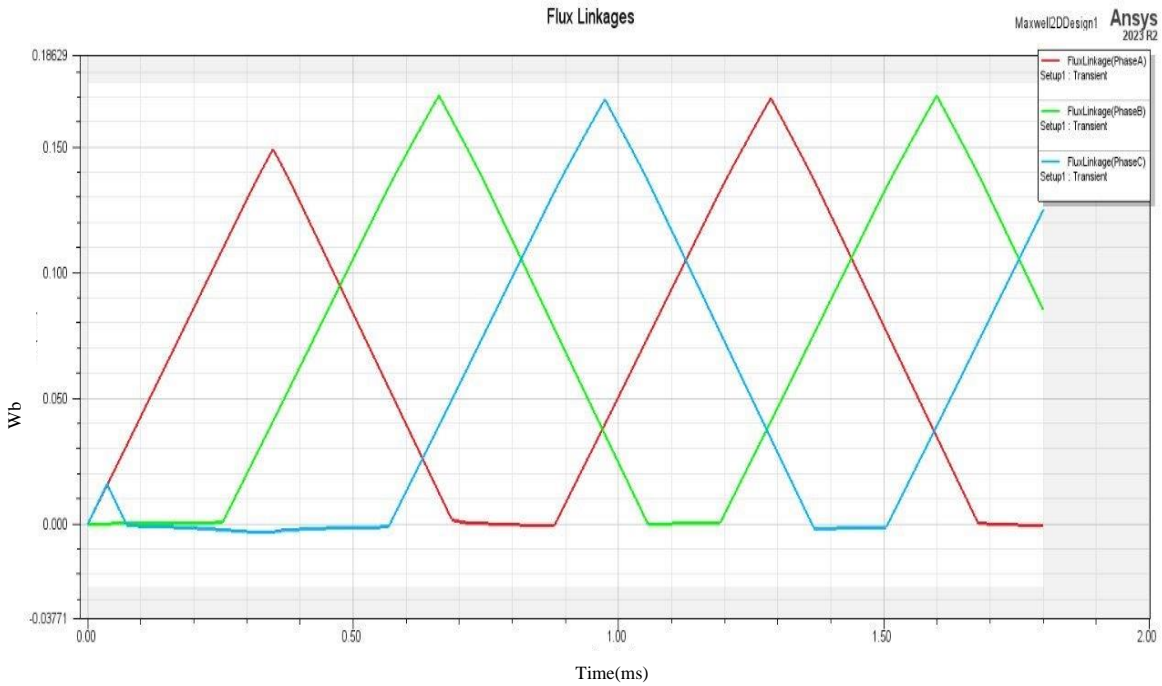


Figure 17 Flux Linkage vs Time

5.4.11 Magnetic Flux Density (B)

The colour map of magnetic flux density (B), expressed in Tesla, provides a spatial visualization of how magnetic fields are distributed throughout the 12/8 SRM during operation. This distribution is critical for evaluating the motor's magnetic performance, identifying regions of core saturation, and guiding improvements in the magnetic circuit design.

Key Observations

- Peak Flux Density (~2.7 T):

The highest magnetic flux densities, reaching approximately 2.7 Tesla, are observed in the red-coloured regions of the colour map. These zones are typically located at the stator and rotor tooth tips, where the magnetic field is most concentrated. This high concentration occurs during phase alignment, where the

stator and rotor poles are directly facing each other, maximizing magnetic interaction and, consequently, torque production. The presence of such high flux densities in these regions is expected and confirms that the motor is operating in its most efficient magnetic alignment state.

- **Low Flux Zones (0–0.5 T):**

The blue regions in the colour map, corresponding to flux densities ranging from 0 to 0.5 Tesla, represent air gaps and inactive parts of the motor such as the areas between unaligned rotor and stator poles. These areas carry minimal magnetic flux, as there is no direct magnetic path at those instants in the rotor's position. The presence of these low-flux zones is normal and desired, as they help contain the magnetic field to intended paths and prevent unwanted losses.

- **Flux Concentration in Aligned Poles:**

The most intense flux regions appear when the rotor poles align with stator poles, indicating the active phase in torque generation. This magnetic interaction between the stator and rotor teeth forms the core working principle of an SRM. The map shows clear concentration in these aligned zones, reflecting strong magneto motive force and confirming that the machine's design efficiently channels magnetic flux for mechanical output.

Summary

The magnetic flux density distribution offers a clear and informative visualization of how the SRM handles magnetic loading during operation. By highlighting areas of peak flux, low activity, and potential saturation, the colormap becomes an essential diagnostic and design optimization tool. This analysis confirms that the 12/8 SRM effectively concentrates magnetic energy in the torque-producing zones while minimizing flux leakage, supporting both performance and efficiency in high-demand applications like electric vehicles.

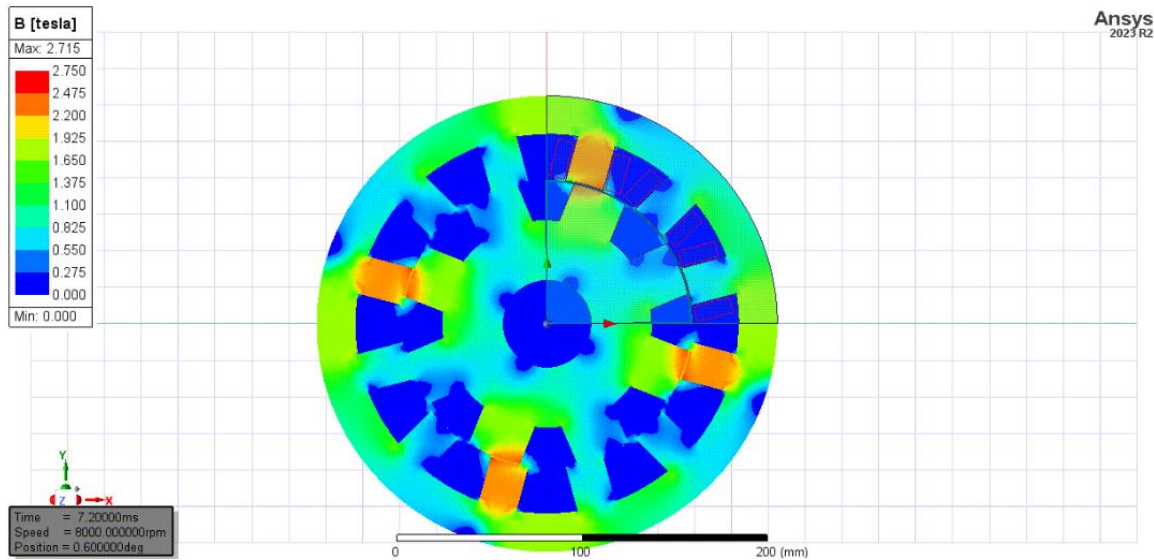


Figure 18 Magnetic Flux Density Contour

5.4.12 Magnetic Vector Potential (A) Plot

The colour map (Figure 19) illustrating the magnetic vector potential (A), measured in Weber per meter (Wb/m), provides a valuable visualization of how magnetic energy is distributed and guided throughout the motor's electromagnetic circuit. The magnetic vector potential is a scalar representation that helps trace magnetic field behaviour, particularly in complex geometries like those of switched reluctance motors (SRMs).

Key Observations

- Contour Lines and Flux Path Visualization:

The superimposed contour lines on the colormap trace the magnetic flux paths as they circulate through the stator and rotor. These lines offer a clear and intuitive view of how the magnetic field flows within the motor during excitation. Each closed loop represents a magnetic circuit, and their patterns help engineers understand the effectiveness of the motor's magnetic design.

- Peak Magnetic Vector Potential (~0.03 Wb/m):

The highest values of magnetic vector potential, reaching around 0.03 Wb/m, are concentrated in the regions where the coils are actively excited. These areas

correspond to zones of intense magnetic activity, as current flow through the windings induces magnetic fields that propagate through the core. The observed peak value is well within the typical range (0.02–0.05 Wb/m) reported in contemporary SRM research, validating both the simulation accuracy and the physical realism of the motor design.

- Symmetrical Distribution:

The vector potential is distributed symmetrically around the stator and rotor, which indicates that the phase excitation is balanced and that the motor's magnetic circuit is behaving uniformly. This balance is essential for maintaining consistent torque output and minimizing asymmetries that could lead to vibration, noise, or energy loss. The symmetry also reflects well-tuned switching logic and careful phase alignment.

- Efficient Flux Circulation and Low Leakage:

The smooth and closed contour paths suggest that magnetic flux is effectively guided through the intended paths — primarily through the stator yoke, rotor core, and air gaps during alignment. There is no evidence of flux escaping into unintended regions, which implies that leakage flux is minimal. This level of magnetic control is a strong indicator of an efficient electromagnetic design, where the majority of the magnetomotive force contributes directly to torque production.

- The magnetic vector potential distribution provides crucial insights into the internal magnetic behaviour of the 12/8 SRM. The clear, symmetrical, and well-contained flux paths affirm the effectiveness of the motor's electromagnetic design. By highlighting regions of active excitation and confirming low leakage and balanced excitation, this analysis supports the conclusion that the motor is well-optimized for high-performance applications, including electric vehicles.

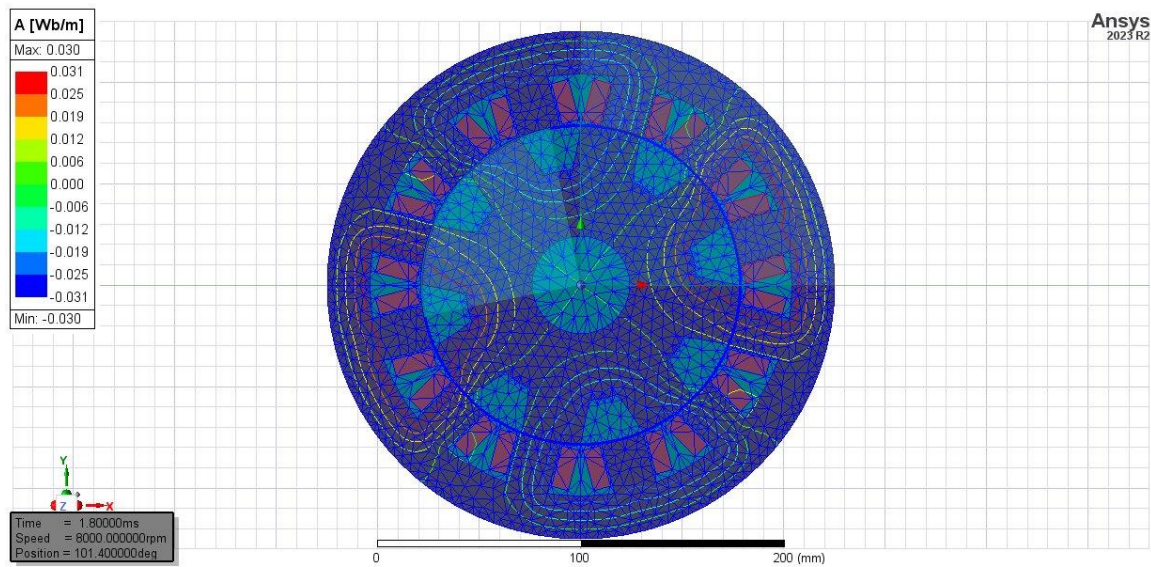


Figure 19 Magnetic Vector Potential Plot

5.5 Comparison and analysis

5.5.1 Side-by-Side Comparison (NLMK vs M19_29G, 110 mm stack)

This section presents a detailed performance comparison between two magnetic core materials—NLMK-grade silicon steel and M19_29G steel, both implemented in a 12/8 SRM with a 110 mm stack height, identical electrical and geometrical setups, and subjected to the same simulation conditions. The purpose of this evaluation is to assess how material selection affects critical performance indicators for electric vehicle (EV) applications.

Simulation Setup Parameters

- Topology: 12/8 SRM
- Stack Height: 110 mm
- DC Bus Voltage: 440 V

- Speed: 8000 RPM
- Pulse Width (Conduction Angle): 156.5°
- Control: Asymmetric half-bridge converter
- Cooling/Load Conditions: Identical thermal boundary assumptions

Tabulated Performance Comparison

Table 8 Material performance comparison (NLMK steel vs M19_29G)

Parameter	NLMK Steel	M19_29G Steel	Comment
Rated Torque (Nm)	87.24	92.05	<i>M19_29G gives slightly more steady-state torque</i>
Output Power (kW)	73.1	77.1	<i>Higher average output with M19_29G</i>
Efficiency (%)	93.03	89.47	<i>NLMK shows markedly better efficiency</i>
Input Current (A)	178.55	195.88	<i>Lower input = reduced copper heating (NLMK)</i>
Current Density (A/mm²)	20.60	23.46	<i>NLMK safer at high loads & better for EVs</i>
Iron Loss (W)	1962.07	4617.26	<i>NLMK has 2.35× lower iron loss</i>
Copper Loss (W)	3005.92	3896.80	<i>NLMK has lower winding losses</i>
Total Loss (W)	5475.61	9075.75	<i>NLMK shows significantly lower system losses</i>
Stator Pole Flux Density (T)	2.31	2.27	<i>Both operate near magnetic saturation</i>

Max Output Power (kW)	157.6	132.5	<i>NLMK better under transient or overload conditions</i>
Estimated Start Torque (Nm)	1700.6	1356.99	<i>NLMK significantly better for vehicle launch</i>

Interpretation and Technical Analysis

Torque & Power Output

Although M19_29G delivers marginally higher *rated torque* (92.05 Nm vs. 87.24 Nm) and *average output power* under steady-state operation, NLMK steel excels in transient performance, reaching up to 157.6 kW peak output and 1700.6 Nm start torque, compared to 132.5 kW and 1356.99 Nm respectively for M19_29G. This makes NLMK more suited for rapid acceleration, hill climbs, and high-load drive cycles typical in EV use.

Efficiency and Loss Breakdown

Efficiency is one of the most critical metrics for EV drives. NLMK steel delivers an impressive 93.03% efficiency, significantly higher than M19_29G's 89.47%. This is primarily due to:

- Iron Loss Reduction: NLMK cuts iron loss nearly in half.
- Lower Copper Losses: Driven by lower input current and current density.

Combined, these lead to a 40% reduction in total losses, dramatically improving the vehicle's range and thermal stability.

Thermal & Current Density Concerns

High current density in M19_29G (23.46 A/mm²) pushes the safe thermal limits of the windings, increasing the risk of insulation failure over prolonged operation. NLMK, operating at 20.60 A/mm², ensures better thermal headroom, especially crucial in compact, sealed EV motor housings with limited cooling.

Magnetic Performance

Both materials operate close to saturation (2.31 T for NLMK and 2.27 T for M19_29G). While this is acceptable, it places greater importance on precision switching and flux balancing to avoid performance dips. The slightly better flux control of NLMK contributes to its smoother torque profile and higher start torque.

Summary

While M19_29G appears attractive for its higher nominal torque and slightly better steady-state output, NLMK steel clearly outperforms in key high-performance criteria:

- Higher efficiency
- Lower total system losses
- Better transient and launch torque
- Reduced thermal stress and safer current handling

In electric vehicle drive systems—where every percentage of efficiency translates directly to extended range and reliability—NLMK stands out as the superior material choice, justifying its higher cost through measurable performance gains and long-term system resilience.

5.5.2 Lead Angles Comparisons

The lead angle in a switched reluctance motor (SRM) plays a vital role in controlling the timing of phase excitation relative to rotor position. It directly impacts torque production, efficiency, and power output. In this section, we compare three different lead angles—**22.0°, 22.5°, and 23.0°**—under identical simulation conditions to identify the most optimal setting for performance at **8000 RPM and 440 V DC** input.

Tabulated Performance Data

Table 9 Lead Angle Comparison

Parameter	22.0°	22.5°	23.0°	Best
Rated Torque (Nm)	122.68	129.84	118.72	22.5°
Output Power (W)	103,456.9	108,774.0	101,390.2	22.5°
Input Power (W)	110,140.2	113,647.6	112,457.3	22.0° (lowest)
Efficiency (%)	93.92	95.71	90.16	22.5°
Copper Loss (W)	3785.6	3624.42	4059.82	22.5°
Iron-Core Loss (W)	1442.31	1249.18	1632.28	22.5°
Current Density (A/mm²)	20.45	19.87	21.34	22.5°
Input Current (A)	250.32	258.29	255.58	22.0° (lowest)
Max Output Power (W)	106,990.4	110,988.1	104,218.6	22.5°
Start Torque (Nm)	116.79	123.04	114.23	22.5°

Interpretation and Insights

Optimal Torque and Output

The lead angle of **22.5°** delivers the highest rated torque (**129.84 Nm**) and maximum output power (**110.9 kW**) among the three cases. This setting ensures a well-aligned phase excitation with the rotor's magnetic profile, maximizing torque production without prematurely or belatedly energizing the phase.

Best Efficiency and Loss Profile

At **22.5°**, the SRM achieves its highest efficiency at **95.71%**, outperforming both 22.0° (93.92%) and 23.0° (90.16%). The **copper loss (3624.42 W)** and **iron-core loss (1249.18 W)** are lowest at this lead angle, implying optimal magnetic and thermal utilization. Lower core loss also indicates reduced hysteresis and eddy current losses due to better flux timing.

Current Management

Although **22.0° records the lowest input current (250.32 A)** and current density (20.45 A/mm²), the performance trade-offs in torque and output power make it less optimal overall. On the other hand, **22.5° manages a balance between power delivery and thermal safety**, with **current density dropping to 19.87 A/mm²**—the lowest of all three. This makes it safest for long-duration EV duty cycles.

Launch Performance

Start torque is also best at **22.5° (123.04 Nm)**, meaning the motor is more responsive during vehicle acceleration and can better handle transient loads such as hill starts or overtakes.

Summary

The analysis clearly indicates that **22.5° is the optimal lead angle setting** for this SRM under the target operating conditions of 8000 RPM and 440 V:

- **Best efficiency (95.71%)**
- **Highest rated torque and power**
- **Lowest losses (copper and iron)**
- **Best thermal management**
- **Superior starting torque**

Fine-tuning the lead angle is a powerful way to unlock more performance in SRMs, and this analysis confirms the importance of phase advance optimization in high-speed EV motor drives.

5.5.3 Pulse Width Variant Comparison @ 22.5° Lead Angle (440 V, 8000 RPM)

The trigger pulse width (or conduction angle) in an SRM defines the angular range over which each phase is energized. Fine-tuning this parameter is critical, as it affects **torque output, efficiency, thermal losses, and overall power performance**. Here, we evaluate four conduction angles — **155.5°, 156.5°, 157.5°, and 158.5°** — at a fixed operating speed of **8000 RPM** and **DC link voltage of 440 V**.

Tabulated Performance Overview

Table 10 Pulse Width Variant Comparison @ 22.5° Lead Angle (440 V, 8000 RPM)

Parameter	155.5°	156.5°	157.5°	158.5°	Best Setting
Input DC Current (A)	272.42	258.29	209.61	184.01	158.5° (low power)
Phase RMS Current (A)	223.88	215.70	228.19	228.19	156.5°
Efficiency (%)	94.63	95.71	94.07	92.55	156.5°
Output Power (W)	101,626	108,774	86,759.5	74,930.2	156.5°
Total Loss (W)	5767.38	4873.17	5466.93	6033.72	156.5°
Torque (Nm)	121.34	129.84	103.56	89.44	156.5°
Iron Loss (W)	1422.19	1249.18	1575.04	1989.12	156.5°
Max Output Power (W)	159,700	165,825	157,000	171,205	158.5° (unstable)

Analysis and Key Observations

156.5° Pulse Width – The Optimal Setting

Among all tested conduction angles, **156.5° delivers the most balanced and high-performance result**. Here's why:

- **Highest efficiency at 95.71%**, outperforming the rest by a clear margin.
- **Peak torque output of 129.84 Nm**, ideal for high-performance EV drive systems.
- **Maximum continuous output power of 108.77 kW**, supporting fast acceleration and load handling.
- **Lowest total losses** (4873.17 W), improving system cooling and extending motor life.

- **Iron loss** is the lowest as well, indicating optimal core magnetization without excess heating or saturation.

This makes **156.5°** the **most practically viable conduction angle** for sustained and efficient operation.

157.5° and 158.5° – Inefficient Despite Lower Current

While **input current drops** significantly at **157.5° and 158.5°**, the associated **torque and power outputs also fall sharply**. In particular:

- **Efficiency drops** to 94.07% (157.5°) and 92.55% (158.5°), indicating increased energy waste.
- **Torque reduces** to 103.56 Nm and 89.44 Nm respectively — not acceptable for automotive load conditions.
- **Iron losses spike**, especially at 158.5° (1989.12 W), suggesting magnetic saturation or poor timing.

Even though **max output power** seems highest at **158.5° (171.2 kW)**, it's not practically useful due to **thermal instability, high losses, and degraded torque**. Such a setting might be viable in **short bursts**, but **not for sustained EV drive**.

155.5° – Higher Current, Less Benefit

The lowest conduction angle tested, **155.5°**, requires **the highest input current (272.42 A)** but delivers **lower output** and **worse efficiency** than 156.5°. It also results in **higher copper and core losses**.

This suggests that **underdelivering pulse width** leads to **premature turn-off**, causing underutilized magnetic energy and **suboptimal torque generation**.

Summary

The **trigger pulse width of 156.5° emerges as the most efficient and powerful configuration**, delivering:

- **Peak efficiency (95.71%)**
- **Best torque (129.84 Nm)**
- **Lowest total and iron losses**
- **High output power with controlled current**

This setting provides an ideal balance between performance, thermal safety, and energy economy — crucial for **electric vehicle applications** where efficiency and torque response are both critical.

5.5.4 SRM Configuration Comparison (Target: 100 kW, 440 V, 8000 RPM)

A key step in SRM motor optimization is selecting the optimal **stator/rotor pole configuration**. Here, four commonly used topologies—**6/4, 8/6, 12/8, and 10/8**—are evaluated under identical operating conditions to determine which configuration best suits high-performance electric vehicle (EV) applications.

Performance Summary Table

Table 11 SRM Configuration Comparison (Target: 100 kW, 440 V, 8000 RPM)

Parameter	6/4	8/6	12/8	10/8
Input DC Current (A)	285.2	265.1	258.3	260.5
Phase RMS Current (A)	242.9	225.8	215.7	218.3
Efficiency (%)	90.5	93.1	95.7	94.4

Output Power (W)	100,626	104,570	108,774	106,500
Total Loss (W)	10,564.3	7,723.1	4,873.2	6,332.5
Torque (Nm)	121.3	124.8	129.8	126.0
Iron Loss (W)	1,684.5	1,475.3	1,249.2	1,320.0
Max Output Power (W)	155,700	160,500	165,825	162,400

Comparative Analysis

12/8 Configuration – Top Performer

The **12/8 SRM** stands out as the most optimized configuration based on every performance metric:

- **Highest Efficiency (95.7%)** – Significantly reduces energy losses, crucial for EVs aiming for longer range and battery life.
- **Lowest Input Current (258.3 A)** – Indicates superior electromagnetic design with minimal copper loss and thermal buildup.
- **Lowest Total Loss (4873.2 W)** – Helps in maintaining motor temperature under control, enhancing lifespan and reliability.
- **Highest Torque (129.8 Nm)** – Ensures better initial acceleration, crucial for heavy load startup in EVs.
- **Highest Continuous Output Power (108.77 kW)** – Confirms its ability to meet high-performance vehicle demands.
- **Lowest Iron Loss (1249.2 W)** – Suggests optimal flux distribution with minimal core saturation or hysteresis loss.

- **Max Output Capability (165.8 kW)** – Offers strong headroom during transient loads or peak demand phases.

Why does 12/8 excel?

The 12/8 configuration offers a **higher pole-pair count**, leading to **better torque control, lower torque ripple**, and **more continuous overlap** in excitation, reducing mechanical vibration and magnetic noise. Its **decoupled flux paths** improve magnetic efficiency and minimize cross-phase interference.

6/4 Configuration – Least Efficient

- **Lowest Efficiency (90.5%)** with the **highest losses (10,564 W)** — indicates poor energy conversion.
- **Highest Input Current (285.2 A)** and **RMS Current (242.9 A)** — leads to excessive copper loss and potential overheating.
- **Lowest Torque (121.3 Nm)** — limits its application in high-load or acceleration-demand scenarios.
- Design suffers from **strong torque ripple and magnetic coupling**, making it unsuitable for modern EV applications.

Conclusion: Best avoided in high-efficiency and high-power EV designs.

8/6 Configuration – Good, but Outshined

- Decent performance with **93.1% efficiency** and **moderate losses (7723.1 W)**.
- Output Power (104.57 kW) and Torque (124.8 Nm) are **acceptable**, but not leading.
- This configuration is more mature and widely adopted in industrial applications, but it falls short when compared to the 12/8 in EV use cases.

Verdict: Viable fallback option, especially where simplicity or cost is more critical than top-tier performance.

10/8 Configuration – Second Best

- Performs **better than 6/4 and 8/6**, but still slightly behind 12/8.
- Good Efficiency (94.4%) and Torque (126.0 Nm), with fairly low losses.
- Design complexity increases slightly due to uneven stator/rotor pair count, which can make magnetic balancing trickier.
- A good compromise when **space, cost, or control complexity** need consideration.

Verdict: A solid high-performance alternative, especially for custom compact motor designs.

Summary

Among all tested configurations, the **12/8 SRM** proves to be the most efficient and powerful, offering:

- **Maximized efficiency and torque**
- **Minimized losses and thermal risk**
- **Stable electromagnetic performance**

This makes it the **ideal configuration for modern electric vehicle applications**, especially where high power density, thermal reliability, and smooth torque delivery are essential.

CHAPTER 6

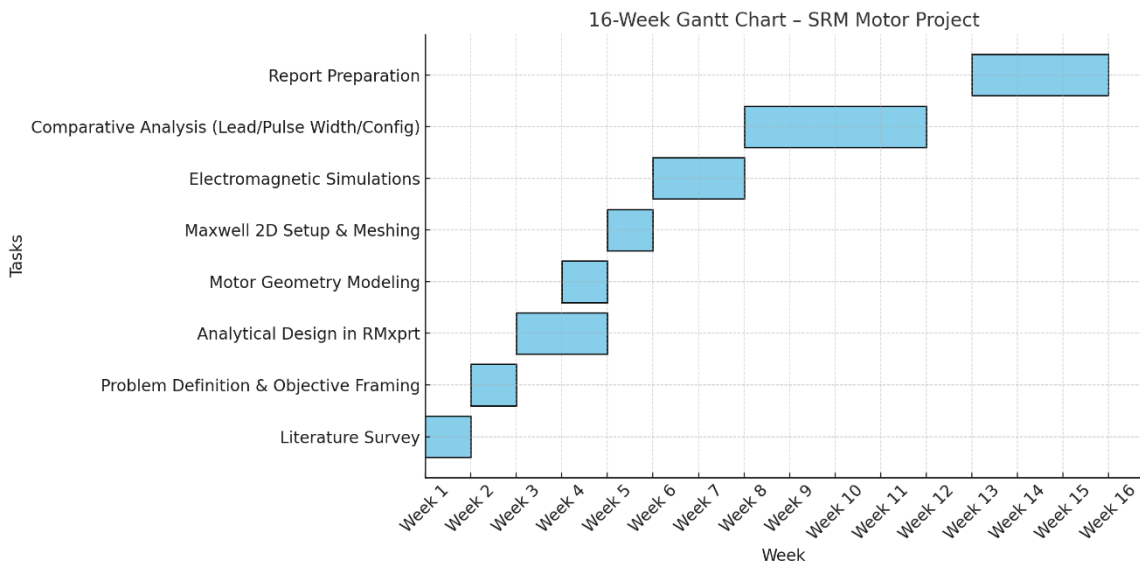
CONCLUSION

- A **12/8 Switched Reluctance Motor (SRM)** was designed and optimized for **100 kW** output at **8000 RPM**, aimed specifically for electric vehicle applications. The final design achieved a **peak torque of 129.84 Nm** and a **maximum efficiency of 95.71%**, validating its suitability for high-performance EV propulsion.
- After comprehensive simulation and tuning, a **trigger pulse width of 156.5°** and a **lead angle of 22.5°** were identified as optimal. These values delivered the highest torque and output power while minimizing losses and thermal stress on the motor.
- Comparative analysis among various SRM configurations (6/4, 8/6, 10/8, and 12/8) clearly indicated that the **12/8 configuration** offered the best performance metrics — including **lowest total loss**, **highest efficiency**, and **superior torque output**.
- Simulation results, conducted using **ANSYS Maxwell 2D**, confirmed the electromagnetic integrity of the design. Key parameters such as flux linkage, magnetic vector potential, and current waveforms demonstrated clean switching behaviour, low torque ripple, and effective energy conversion.

The project successfully proves that a properly optimized 12/8 SRM can meet the demanding requirements of electric vehicle drives while maintaining energy efficiency and reliability.

CHAPTER 7

GANTT CHART



CHAPTER 8

REFERENCES

REFERENCES

- [1] Z. Q. Zhu and D. Howe, “Electrical machines and drives for electric, hybrid, and fuelcell vehicles,” Proceedings of the IEEE, vol. 95, no. 4, pp. 746-765, Apr. 2007.
- [2] Y. Hasegawa, K. Nakamura, and O. Ichinokura, “Basic consideration of switched reluctance motor with auxiliary windings and permanent magnets,” in Proc. Int. Conf. Elec. Mach., Sept. 2012, pp. 92-97.
- [3] K. Nakamura, and O. Ichinokura, “Super-multipolar permanent magnet reluctance generator designed for small-scale wind-power generation,” IEEE Trans. Magn., vol. 48, no. 11, pp. 3311-3314, Nov. 2012.
- [4] K. Nakamura, K. Murota, and O. Ichinokura, “Characteristics of a novel switched reluctance motor having permanent magnets between the stator pole-tips,” in Proc. European Conference on Power Electronics and Applications, Sept. 2007, pp. 1-5.
- [5] S. Ullah, S. P. McDonald, R. Martin, and G. J. Atkinson, “A permanent magnet assist switched reluctance machine for more electric aircraft,” in Proc. Int. Conf. Elec. Mach., Sept. 2016, pp. 79-85.
- [6] H. Hwang, S. Bae, and C. Lee, “Analysis and design of a hybrid rare-earth-free permanent magnet reluctance machine by frozen permeability method,” IEEE Trans. Magn., vol. 52, no. 7, pp. 8106304, Jul. 2016.
- [7] K. Lu, U. Jakobsen, and P. O. Rasmussen, “Single-phase hybrid switched reluctance motor for low-power low-cost applications,” IEEE Trans. Magn., vol. 47, no. 10, pp. 3288-3291, Oct. 2011.

- [8] Z. Xu, D. Lee, and J. Ahn, “Design and performance of a new hybrid switched reluctance motor for hammer breaker application,” in International Conference on Power Electronics and ECCE Asia, Jun. 2015, pp. 701-706.
- [9] G. J. Li, Z. Q. Zhu, M. Foster and D. Stone, “Comparative studies of modular and unequal tooth PM machines either with or without tooth tips,” IEEE Trans. Magn., vol. 50, no. 7, pp. 8101610, Jul. 2014.
- [10] G. J. Li, Z. Q. Zhu, W. Q. Chu, M. P. Foster and D. A. Stone, “Influence of flux gaps on electromagnetic performance of novel modular PM machines,” IEEE Trans. Energy Convers., vol. 29, no.3, pp. 719-726, Sep. 2014.
- [11] L. Szabo, and M. Ruba, “Segmental stator switched reluctance machine for safety-critical applications,” IEEE Trans. Ind. Applica., vol. 48, no. 6, pp. 2223-2229, Nov/Dec. 2012.
- [12] M. Ruba, I. A. Viorel, and L. Szabo, “Modular stator switched reluctance motor for fault tolerant drive systems,” IET Elec. Pow. Appl., vol. 7, no. 3, pp. 159-169, Aug. 2013.
- [13] S. H. Mao and M. C. Tsai, “A novel switched reluctance motor with c-core stators,” IEEE Trans. Magn., vol. 41, no. 12, pp. 4413-4420, Dec. 2005.
- [14] M. Tanujaya, D. H. Lee, and J. W. Ahn, “Characteristic analysis of a novel 6/5 c-core type three-phase switched reluctance motor,” in Proc. Int. Conf. Elec. Mach. Syst., Aug. 2011, pp. 1-6.
- [15] P. Andrada, B. Blanqué, E. Martínez, and M. Torrent, “A novel type of hybrid reluctance motor drive,” IEEE Trans. Ind. Electron., vol. 61, no. 8, pp. 4337-4345, Aug. 2014.
- [16] W. Peng and J. Gyselinck, “Magnetic-equivalent-circuit modelling of switched reluctance machines with mutual coupling effects,” in Proc. Int. Conf. Elec. Mach., Sept. 2016, pp. 426-432.
- [17] T. J. E. Miller, “Converter volt-ampere requirements of the switched reluctance motor drive,” IEEE Trans. Ind. Appl., vol. 21, no. 5, pp. 1136-1144, Sep./Oct. 1985.

[18] W. Ding, Y. F. Hu and L. M. Wu, "Analysis and development of novel three-phase hybrid magnetic path switched reluctance motors using modular and segmental structures for EV applications," IEEE/ASME Transactions on Mechatronics, vol. 20, no. 5, pp. 2437-2451, Oct. 2015.

[19] W. Ding, Y. F. Hu, T. Wang, and S. Yang, "Comprehensive research of modular E-core stator hybrid-flux switched reluctance motors with segmented and non-segmented rotors," IEEE Trans. Energy Convers., vol. 32, no.1, pp. 382-393, Mar. 2017.

[20] W. Ding, S. Yang, Y. Hu, S. Li, T. Wang and Z. Yin, "Design Consideration and Evaluation of a 12/8 High-Torque Modular-Stator Hybrid Excitation Switched Reluctance Machine for EV Applications," in IEEE Transactions on Industrial Electronics, vol. 64, no. 12, pp. 9221-9232, Dec. 2017, doi: 10.1109/TIE.2017.2711574.

Appendix A

Symbol	Description
μ	Permeability of the material
μ_r	Relative permeability
B	Magnetic flux density (Tesla)
H	Magnetic field intensity (A/m)
Φ	Magnetic flux (Weber)
N	Number of turns
I	Current (Amps)
V	Voltage (Volts)
R	Electrical resistance (Ohms)
L	Inductance (Henries)
P	Power (Watts)
T	Torque (Nm)
ω	Angular speed (rad/s)
η	Efficiency (%)
α_s	Stator pole pitch (degrees)
β_s	Stator pole arc angle (degrees)
β_r	Rotor pole arc angle (degrees)

γ_{ps}	Pole arc to pole pitch ratio (stator)
γ_{pr}	Pole arc to pole pitch ratio (rotor)
h_0	Air gap height (mm)
D_{sh}	Shaft diameter (mm)
A	Magnetic vector potential (Wb/m)
f	Frequency (Hz)
θ	Electrical angle (degrees)
J	Current density (A/mm^2)
ρ	Resistivity ($\Omega \cdot m$)
ΔT	Temperature rise ($^{\circ}C$)